Cytokinin-CLAVATA crosstalk is an ancient mechanism regulating shoot meristem homeostasis in land plants

Joseph Cammarata1,2,3, Christopher Morales Farfan1,2, Michael Scanlon1*, and Adrienne HK Roeder1,2*

1. School of Integrative Plant Science, Section of Plant Biology, Cornell University, Ithaca, NY 14853

2. Weill Institute for Cell and Molecular Biology, Cornell University, Ithaca, NY 14853

3. Department of Biology, Duke University, Durham, NC 27708 (present address)

* Authors for correspondence: mjs298@cornell.edu, ahr75@cornell.edu

Abstract

Plant shoots grow from stem cells within Shoot Apical Meristems (SAMs), which produce lateral organs while maintaining the stem cell pool. In the model flowering plant Arabidopsis, the CLAVATA (CLV) pathway functions antagonistically with cytokinin signaling to control the size of the multicellular SAM via negative regulation of the stem cell organizer WUSCHEL (WUS). Although comprising just a single cell, the SAM of the model moss *Physcomitrium patens* (formerly *Physcomitrella*) performs equivalent functions during stem cell maintenance and organogenesis, despite the absence of WUS-mediated stem cell organization. Our previous work showed that the stem cell-delimiting function of the receptors CLAVATA1 (CLV1) and RECEPTOR-LIKE PROTEIN KINASE2 (RPK2) is conserved in the moss *P. patens*. Here, we use *P. patens* to assess whether CLV-cytokinin crosstalk is also an evolutionarily conserved feature of stem cell regulation. Application of cytokinin produces ectopic stem cell phenotypes similar to *Ppclv1a Ppclv1b* and *Pprpk2* mutants. Surprisingly, cytokinin receptor mutants also form ectopic stem cells in the absence of cytokinin signaling. Through modeling, we identified regulatory network architectures that recapitulated the stem cell phenotypes of *Ppclv1a Ppclv1b* and *Pprpk2* mutants, cytokinin application, cytokinin receptor mutations, and higher-order combinations of these perturbations. These models predict that *Pp*CLV1 and *Pp*RPK2 act through separate pathways wherein *Pp*CLV1 represses cytokinin-mediated stem cell initiation and *Pp*RPK2 inhibits this process via a separate, cytokinin-independent pathway. Our analysis suggests that crosstalk between CLV1 and

cytokinin signaling is an evolutionarily conserved feature of SAM homeostasis that preceded the role of WUS in stem cell organization.

Introduction

Plant shoot morphology is generated by pluripotent stem cells called Shoot Apical Meristems (SAMs) at growing shoot tips. SAMs perform two essential functions during morphogenesis: to pattern lateral organ initiation and to maintain the stem cell population by replacing cells differentiated during organogenesis. Decades of study in the model flowering plant *Arabidopsis thaliana* have revealed a key role for a negative feedback loop in SAM homeostasis[1]. Stem cells at the apex of the meristem secrete a slew of CLAVATA3/EMBRYO SURROUNDING REGION (CLE) peptides including CLV3[2,3]. CLV3 acts through a suite of leucine-rich repeat receptor-like kinases (LRR-RLKs) including CLAVATA1 (CLV1) and RECEPTOR-LIKE PROTEIN KINASE2 (RPK2) to repress the expression of the stem cell organizing gene *WUSCHEL* (*WUS*), thereby limiting the size of the stem cell pool[4–8]. WUS promotes expression of *CLV3*, completing the negative feedback loop[9,10]. In Arabidopsis, *wus* mutants fail to maintain a SAM[11,12]. In contrast, *clv3*, *clv1*, or *rpk2* loss-of-function mutants fail to downregulate *WUS* expression and produce too many stem cells, leading to an enlarged and fasciated SAM, increased organ numbers, and stem swelling[1,4].

Unlike the multicellular SAM of flowering plants, the moss SAM comprises a single tetrahedral stem cell[13]. Despite this anatomical difference, the moss apical cell accomplishes the same two essential SAM functions: lateral organ patterning and self-maintenance. In so doing, the moss SAM divides asymmetrically to form a phyllid (leaf-like organ) progenitor cell and a new apical stem cell. The apical division plane rotates to produce phyllids in a spiral pattern around the haploid gametophore (haploid shoot). The transcriptome of the moss SAM shares a high degree of overlap with flowering plant SAMs, suggesting possible deep homology underlying SAM function despite the fact that the moss haploid SAM and the diploid SAM of flowering plants reside in non-homologous shoots[14].

In contrast to flowering plants, the moss *Physcomitrium patens* (previously known as *Physcomitrella patens*) encodes only three orthologs of stem cell-regulating LRR-RLKs: *PpCLV1a*, *PpCLV1b*, and *PpRPK2*. This relative simplicity makes *P. patens* an appealing model for understanding the role of these receptors in stem cell specification[15]. We previously characterized the function of *CLV1* and *RPK2* orthologs in *P. patens* and found that these genes performed similar developmental functions in flowering plants and *P. patens*[16], including regulation of SAM homeostasis. *Ppclv1a Ppclv1b* double mutants and *Pprpk2* single mutants produce ectopic stem cells, suggesting that the canonical roles of CLV1 and RPK2 to reduce stem cell number are conserved. *Pp*CLV1a and *Pp*CLV1b function redundantly[16], so we refer to their combined activity as *Pp*CLV1. Interestingly, whereas the Arabidopsis *clv1* and *rpk2* stem cell phenotypes are attributed to overaccumulation of WUS, *P. patens* lacks this *WUS* function[17]. The *P. patens* genome encodes three *WUSCHEL-RELATED HOMEOBOX* (*WOX*) genes, all of which lack domains critical for the stem cell modulatory function of WUS[17–19]. *P. patens wox* mutants exhibit defective tip-growth in regenerating protonemal filaments, however, gametophore development is normal[20]. Together, these data suggest that *P. patens WOX* genes do not function during SAM homeostasis[20]. This raises the question: in the absence of WOX-mediated stem cell maintenance, how do *Pp*CLV1 and *Pp*RPK2 inhibit stem cell specification in *P patens*?

The hormone cytokinin promotes SAM formation in both Arabidopsis and *P. patens*[30]. Several lines of evidence suggest an antagonistic relationship between CLV1 and RPK2, and cytokinin[16,21]. In *P patens* gametophores, cytokinin promotes the formation of new SAMs[22], while loss of *Pp*CLV1 or *Pp*RPK2 signaling causes ectopic stem cell formation[16]. Intriguingly, in Arabidopsis, cytokinin promotes SAM formation via induction of *WUS* expression[23,24]. This again begs the question of how cytokinin promotes SAM formation in *P patens*, despite the absence of WOX function during stem cell organization. In this study, we ask if there is crosstalk between *Pp*CLV1, *Pp*RPK2, and cytokinin signaling during stem cell specification in *P. patens*.

Mathematical models representing competing hypotheses were fit to the empirical data on SAM homeostasis in wild type versus *Ppclv1a Ppclv1b* and *rpk2* mutant gametophores, with and without cytokinin treatment, and when cytokinin signaling is lost. Maximum support was found for a model where *Pp*CLV1 signaling is upstream of cytokinin-mediated stem cell induction, and *Pp*RPK2 signaling acts via a separate pathway. Overall, our data support a network in which *Pp*CLV1 and cytokinin signaling converge on the regulation of *P. patens* SAM maintenance. This network is distinct from the canonical angiosperm network in that it lacks a role for a *WOX* gene as the hub linking cytokinin and CLV1 pathways. Thus our work suggests crosstalk between CLV1 receptors and cytokinin signaling is an evolutionarily-conserved feature of SAM homeostasis that preceded the role of WUS in stem cell organization.

RESULTS

*Pp*CLV1 and *Pp*RPK2 function through distinct pathways

Our previous research revealed a conserved role for the *P patens* LRR-RLKs *Pp*CLV1A, *Pp*CLV1B, and *Pp*RPK2 in inhibiting stem cell identity in gametophores[16]. Loss of function mutations in the two *PpCLV11a* and *PpCLV1b* paralogs or in *PpRPK2* resulted in gametophores with ectopic apical cells along the lengths of swollen stems[16]. In order to determine whether *Pp*CLV1 and *Pp*RPK2 function in the same pathway to regulate stem cell formation, we used CRISPR-Cas9 mediated mutagenesis to target *PpRPK2* in a *Ppclv1a Ppclv1b* double mutant background and generated three independent, triple mutant lines with the same phenotypes (Supplemental Figure 1). We examined wild type, *Ppclv1a Ppclv1b*, *Pprpk2*, and *Ppclv1a Ppclv1b Pprpk2* mutant gametophores across three developmental timepoints ranging from less than one week old to approximately four weeks old (Figure 1).

Wild-type gametophores were mostly covered with phyllids, leaving little exposed stem tissue (Figure 1 A, B, C). In contrast, the stems of *Ppclv1a Ppclv1b*, *Pprpk2,* and *Ppclv1a Ppclv1b Pprpk2* mutants were swollen from the earliest stages of development (Figure 1D, G, J). Ectopic apical cells were present on the rounded stems of these mutants at all stages of development. Apical cells were identified by the characteristic triangular shape of their apical surface: the top of the tetrahedron. At later stages, *Ppclv1a*

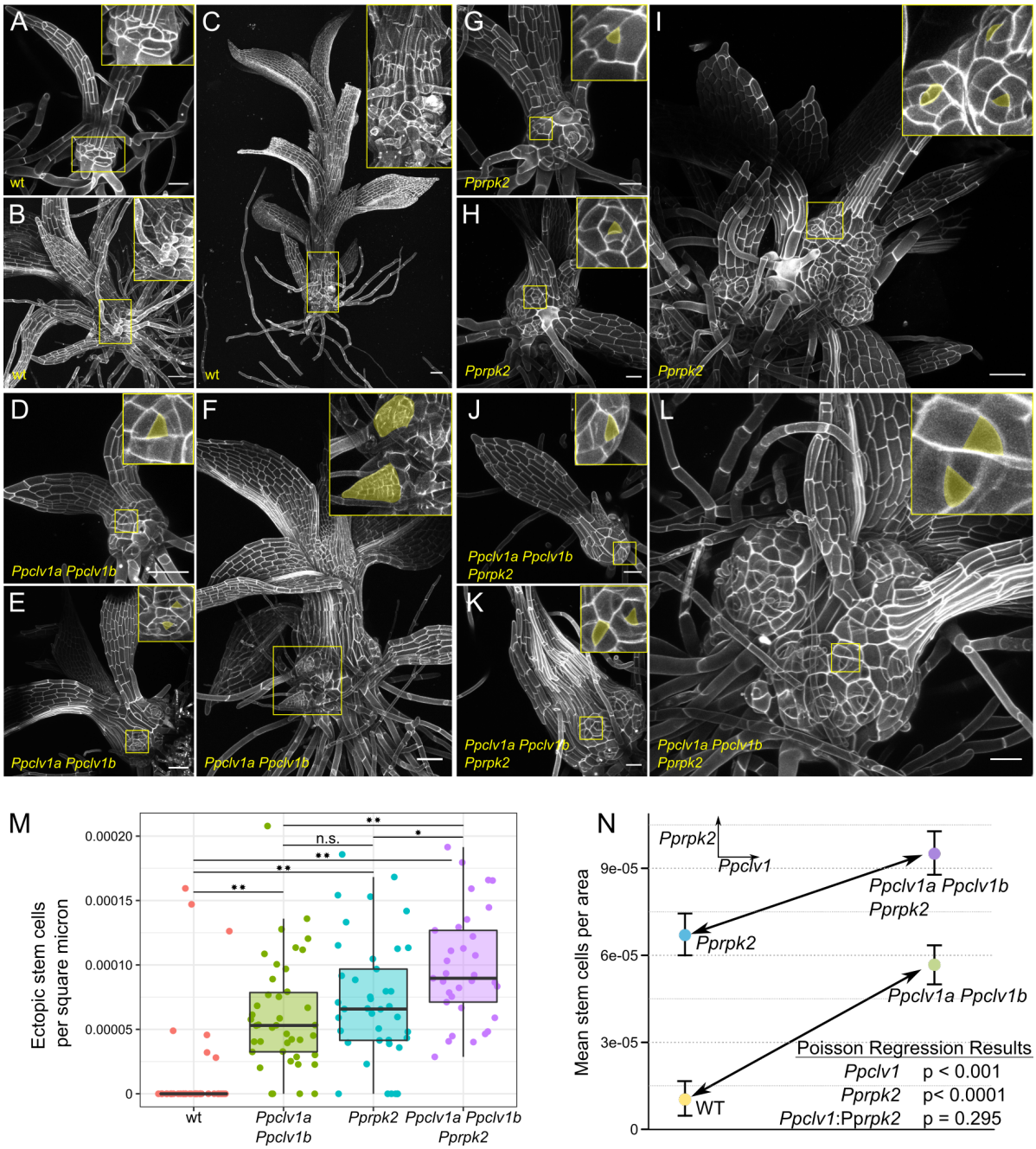

Figure 1: *Ppclv1a Ppclv1b* and *Pprpk2 mutant* phenotypes are additive. Gametophore development at approximately one week (A, D, G, J), two weeks (B, E, H, K) and three to four weeks (C, F, I, L) in wild type (A-C), *Ppclv1a Ppclv1b* (D-F), *Pprpk2* (G-I), and *Ppclv1a Ppclv1b Pprpk2* (J-L). Insets show cells at the base, with ectopic stem cells and outgrowths initiating from stem cells (pseudo colored yellow) in the mutants. (M) Ectopic stem cells per μm^2 of stem tissue from 30 - 40 shoots of each genotype. One star denotes $p < 0.05$; two stars $p < 0.001$; two-sided t-test with Bonferroni correction for multiple testing. (N) An interaction plot showing the effects of *Ppclv1* (left to right, arrow) and *Pprpk2* (top to bottom) mutations on ectopic stem cell per μm^2. The similar slopes of the two lines demonstrate that the effect of the two *Ppclv1* mutations is the same in wild type and *Pprpk2* genetic backgrounds. Results for a Poisson regression testing for significant effects from *Ppclv1a Ppclv1b* mutants, *Pprpk2* mutants, and an interaction between the two are given. Scalebar 50 µm.

Ppclv1b, Pprpk2, and *Ppclv1a Ppclv1b Pprpk2* mutant gametophores produced ectopic phyllids, indicating that the ectopic apical cells observed at earlier stages were indeed functional SAMs (Figure 1F).

All mutant gametophores stopped elongating earlier than the wild type, often terminating in a swollen apex with abundant apical cells (Figure 2). After terminating longitudinal growth, *Ppclv1a Ppclv1b*, *Pprpk2*, and *Ppclv1a Ppclv1b Pprpk2* mutant gametophores continued to swell and initiate new growth axes from ectopic stem cells along the length of the stem (Figure 1 F, I, L, Figure 2). The swelling of gametophore tips in a mass of stem cells in *Ppclv1a Ppclv1b* and *Pprpk2* mutant stems was reminiscent of stem cell over-proliferation and SAM disorganization seen in Arabidopsis *clv* and *rpk2* mutants[4,25], again highlighting the conserved function of this pathway in SAM homeostasis[16].

However, it was not clear how *Pp*CLV1 and *Pp*RPK2 signaling interact to inhibit ectopic stem cell formation. To determine whether *Pp*CLV1 and *Pp*RPK2 function in the same linear pathway, we quantified the number of visible ectopic stem cells by confocal microscopy on 30 - 40 gametophores of each genotype. Gametophores initiate continuously from a *P. patens* tuft, making the age of the tuft a poor indicator of gametophore age. To control for variation in gametophore age and any increase in stem cell count due to increased mutant stem size, ectopic stem cell number was normalized to the size of the stem (Figure 1 M, non-normalized data Supplemental Figure 2). Ectopic stem cells were observed on almost all *Ppclv1a Ppclv1b* and *Pprpk2* gametophores, in contrast with wild type.

If *Pp*CLV1 and *Pp*RPK2 act in a linear genetic pathway, epistasis is predicted in *Ppclv1a Ppclv1b Pprpk2* triple mutants. In contrast, if *Pp*CLV1 and *Pp*RPK2 have redundant functions but act in distinct complexes, a synergistic increase in stem cell initiation is predicted in triple mutants. Finally, if *Pp*CLV1 and *Pp*RPK2 act non-redundantly, i.e. in distinct signaling pathways, additive effects on stem cell initiation phenotypes are expected. The number of ectopic stem cells per area was significantly higher in *Ppclv1a Ppclv1b Pprpk2* triple mutants than either *Ppclv1a Ppclv1b* double mutants ($p < 0.001$) or *Pprpk2* single mutants ($p = 0.01$) (Figure 1 M). An interaction plot revealed that the effect of mutating *PpCLV1a and PpCLV1b* is similar in wild type or *Pprpk2* mutant backgrounds (the slope of the lower and upper lines, respectively) ;

thus, the effects of the *Ppclv1a/Ppclv1b* and *Pprpk2* mutations appear additive (Figure 1 N). A Poisson regression, which is suited for low count data (such as number of ectopic ACs) and included stem area as an offset to control

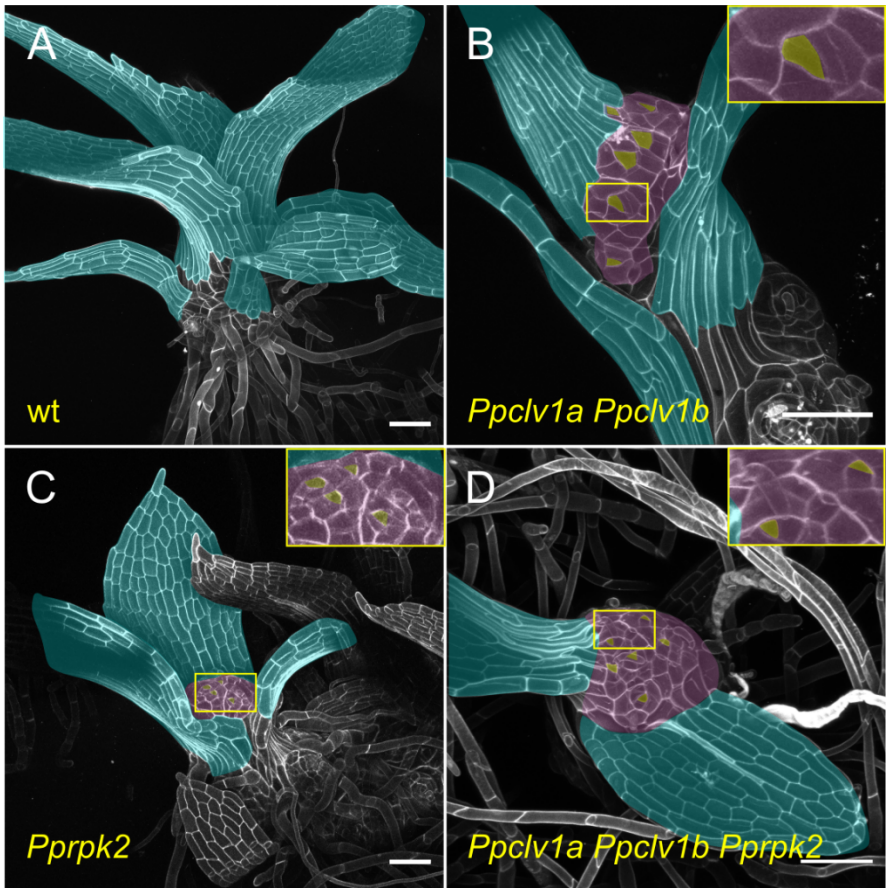

Figure 2: ***Ppclv1a Ppclv1b, Pprpk2,* and *Ppclv1a Ppclv1b Pprpk2* gametophores terminate in a mass of stem cells**. Approximately three-week-old wild type (A), *Ppclv1a Ppclv1b* (B), *Pprpk2* (C), and *Ppclv1a Ppclv1b Pprpk2* mutant (D) gametophores. Bare apices (pseudo colored purple) replete with stem cells (pseudo colored yellow) are visible in *Ppclv1a Ppclv1b*, *Pprpk2,* and *Ppclv1a Ppclv1b Pprpk2* mutants, while the single apical cell at the apex of wild type shoots is well-covered by phyllids (pseudo colored blue). stem cell Scalebars: 100 µm.

for stem size, was used to assess the statistical significance (p-value) and impact (coefficient) of mutating *PpCLV1a/PpCLV1b* and *PpRPK2* and the interaction between these two (Figure 1 N). The regression revealed significant effects for loss of PpCLV1 and PpRPK2 function ($p < 0.0001$ for each and coefficients 0.5054 and 0.6358 for *Ppclv1a/Ppclv1b* and *Pprpk2*, respectively, see supplemental Materials and Methods

for details), but no significant interaction between them (p = 0.29, coefficient -0.1774). In summary, the genetic data suggest that *Pp*CLV1 and *Pp*RPK2 do not function in the same linear pathway during regulation of stem cell abundance in the gametophore.

*Pp*CLV1 and *Pp*RPK2 signalling interactions with Cytokinin signaling

Exogenous cytokinin application induces swelling and the stem cell formation along wild-type gametophores[22], similar to phenotypes observed in *Ppclv1a Ppclv1b* and *Pprpk2* mutants (Figure 3A-C and Figure 1). We hypothesized two possible pathways to explain the convergence of these phenotypes. First, *Pp*CLV1 and/or *Pp*RPK2 could function by inhibiting cytokinin-mediated stem cell specification, i.e. *Pp*CLV1/*Pp*RPK2 function is upstream of cytokinin response. Alternatively, cytokinin signaling might be upstream and inhibit *Pp*CLV1/*Pp*RPK2 function, such that cytokinin de-represses stem cell formation. To better understand how *Pp*CLV1 or *Pp*RPK2 signaling interact with cytokinin signaling, we characterized the response of *Ppclv1a Ppclv1b*, *Pprpk2*, and *Ppclv1a Ppclv1b Pprpk2* mutants to exogenous treatment (10 nM and 100 nM) of the synthetic cytokinin 6-benzylamino purine (BAP). If *Pp*CLV1 or *Pp*RPK2 function upstream or independently of cytokinin signaling, BAP treatment is predicted to induce stem cell formation in *Ppclv1a Ppclv1b* and *Pprpk2* mutants. On the other hand, if cytokinin is an upstream inhibitor of *Pp*CLV1 and/or *Pp*RPK2 function, BAP treatment is expected to have no effect on the *Ppclv1a Ppclv1b* or *Pprpk2* mutant phenotypes.

We quantified the number of ectopic stem cells in each genotype grown on 10 nM and 100 nM cytokinin, normalized to stem area as described above. Wild-type gametophores grown on 10 nM BAP displayed slight swelling and developed ectopic tetrahedral apical cells reminiscent of those seen in *Ppclv1a PPclv1b* and *Pprpk2* mutants (Figure 3A-B). A higher concentration of cytokinin induced swollen stems and numerous outgrowths derived from ectopic stem cells in wild-type plants (Figure 3C, M). In comparison, 10 nM BAP had mild effects on stem swelling and ectopic apical cell formation in *Ppclv1a Ppclv1b* and *Pprpk2* mutant gametophores (Figure 3 E, H, M), although treatment with 100 nM BAP induced numerous ectopic apical cells and a high degree of stem swelling (Figure 3F, I, M). Interestingly, growing *Ppclv1a*

Ppclv1b Pprpk2 mutants on 10 nM or 100 nM BAP resulted in a similar amount of stem cells per area (Figure 3 K, L, M, non-normalized data Supplemental Figure 3), suggesting ectopic stem cell formation was already saturated. Overall, stem cell formation increased in *Ppclv1a Ppclv1b, Pprpk2*, and *Ppclv1a Ppclv1b Pprpk2* mutants in response to cytokinin. These data support a role *Pp*CLV1 and *Pp*RPK2 upstream or independent of cytokinin response.

Interestingly, while cytokinin induced stem cell formation in all genotypes, this effect appeared weaker in *Ppclv1a Ppclv1b* and *Pprpk2* mutants than in wild type (Figure3 M). To statistically assess how *Pp*CLV1, *Pp*RPK2, and cytokinin interact to control stem cell specification, we analyzed our full dataset, comprising each genotype with and without BAP treatment, using a Poisson regression. Notably, there remained a significant increase in stem cells caused by loss of *Pp*CLV1 or *Pp*RPK2 function, as well as cytokinin treatment (p-value and Poisson coefficient for *clv1*: $p = 0.0001$, coefficient = 0.64; *rpk2*: $p < 0.0001$, coefficient = 0.96; cytokinin treatment: $p < 0.0001$, coefficient = 0.0133,). In agreement with our conclusion from Figure 1, cytokinin treatment also revealed no significant statistical interactions between the effects of *Ppclv1a/Ppclv1b* and *Pprpk2* mutations ($p = 0.240$), indicating that these mutant phenotypes are indeed additive. Interestingly, each mutant showed a slight but statistically significant reduced induction of stem cells in response to exogenous cytokinin compared to wild type (Figure 2I*; Ppclv1a Ppclv1b*:cytokinin $p = 0.033$, coefficient = -0.003; *Pprpk2*:cytokinin $p < .0001$; coefficient = -0.009;).

In summary, the phenotypes of *Ppclv1a Ppclv1b* and *Pprpk2* were additive across a range of exogenous cytokinin concentrations, suggesting that *Pp*CLV1 and *Pp*RPK2 act via distinct pathways regulating stem cell specification. Cytokinin increases stem cell initiation in *Ppclv1a Ppclv1b* and *Pprpk2* mutants, supporting a role for *Pp*CLV1 and *Pp*RPK2 upstream or independent of cytokinin signaling. However, loss of *Pp*CLV1 or *Pp*RPK2 function also slightly diminished the effect of exogenous cytokinin on stem cell production. These data suggest that cytokinin response could already be high in *Ppclv1a Ppclv1b* and *Pprpk2* mutants such that exogenous cytokinin treatments represented a smaller relative increase in

cytokinin signaling in the mutants than in wild type. Such a scenario would occur if *Pp*CLV1 and/or *Pp*RPK2 functioned by inhibiting cytokinin-mediated stem cell specification.

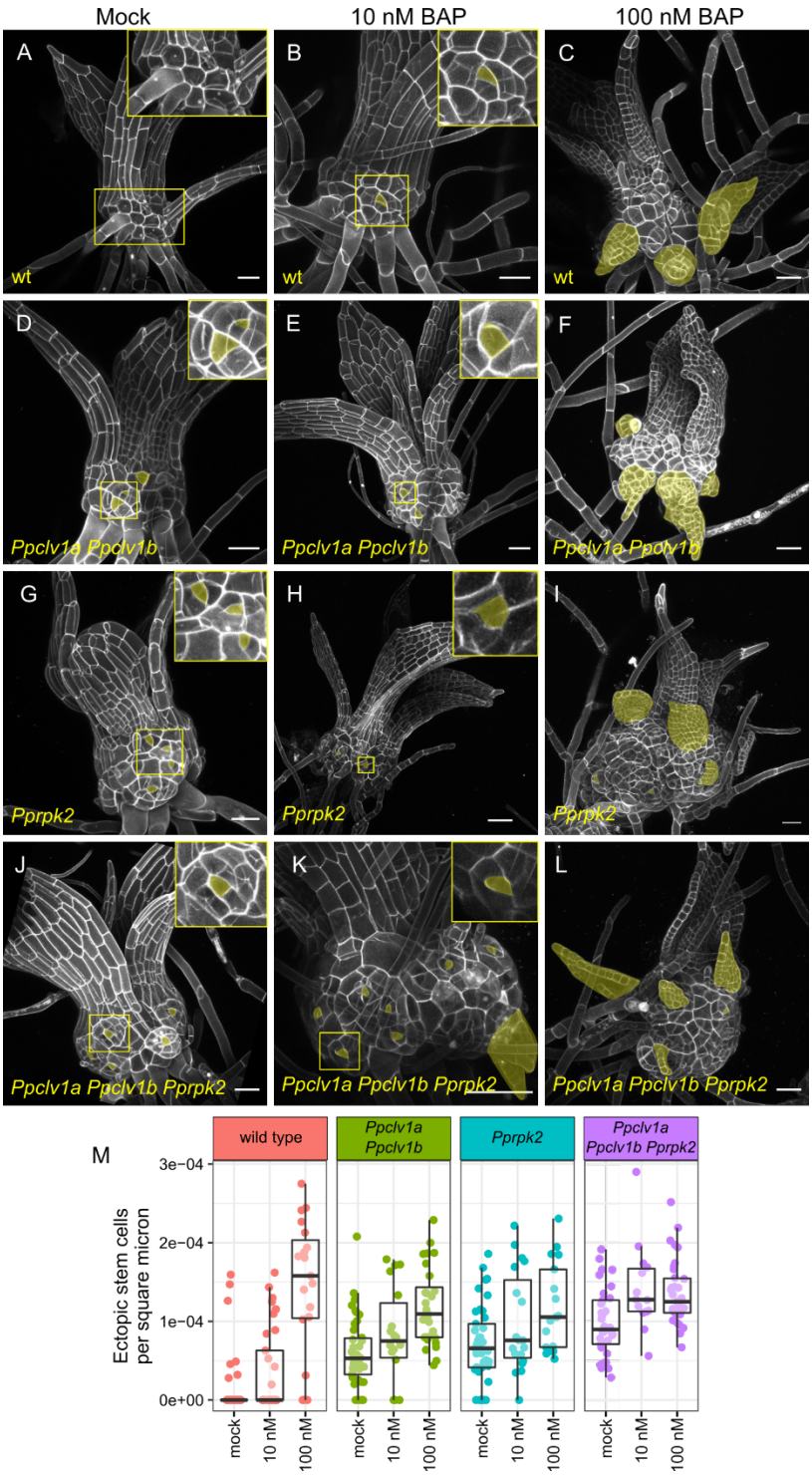

Figure 3: **Cytokinin induces phenotypes similar to *Ppclv1a Ppclv1b* / *Pprpk2* and increases apical cell formation in *Ppclv1a Ppclv1b*/*Pprpk2* mutants.** Two- to three-week-old gametophores grown on mock media

(0 nM A, D, G, J) or media supplemented with low (10 nM, B, E, H, K) or high (100 nM, C, F, I, L) BAP. (M) Quantification of ectopic stem cells per area of exposed stem. Note that (M) includes data from Figure 1M for clarity. Ectopic stem cells and ectopic phyllids (indicative of underlying stem cells) are pseudo colored yellow. Scalebars: 50 µm. See results section for statistics from Poisson regression.

Mathematical modelling supports action by *Pp*CLV1 and *Pp*RPK2 through distinct pathways

To test possible regulatory network topologies that integrate *Pp*CLV1, *Pp*RPK2, and cytokinin signaling to control stem cell identity in gametophores, we evaluated a range of hypothetical gene regulatory network models (e.g. Figure 4 A). Given that the data supported *Pp*CLV1 and *Pp*RPK2 signaling through separate pathways, we coded two variables, 'x' and 'y', to represent two hypothetical pathways each capable of promoting stem cell formation. It is important to note that x and y do not represent any specific genes, but rather are simplified representations of unknown but postulated signaling outputs. As cytokinin induces stem cell formation, we specified that pathway x denotes cytokinin response, while pathway y represents cytokinin-independent stem cell specification pathways.

In the first model, *Pp*RPK2 and *Pp*CLV1 are capable of inhibiting stem cell initiation through both cytokinin-dependent and independent pathways, i.e. through both x and y (Figure 4 A). This model has the greatest flexibility and represents a scenario where PpCLV1 and PpRPK2 have overlapping but non-identical contributions to both the x and y pathways. The second and third models simulate the cases where *Pp*CLV1 and *Pp*RPK2 act completely independently (Figure 4 B and C). In model two, *Pp*CLV1 inhibits cytokinin-mediated stem cell induction (x) and *Pp*RPK2 inhibits cytokinin-independent stem cell induction (y), while the roles for *Pp*CLV1 and *Pp*RPK2 are reversed in model three. As an additional test of whether *Pp*CLV1 and *Pp*RPK2 might be redundant, we included models four and five wherein each inhibits x (Figure 4 D) or y (Figure 4 E) exclusively, although with potentially different strengths. Thus, these five models represent five competing hypotheses where *Pp*CLV1 and *Pp*RPK2 are partially redundant, completely independent, or completely redundant, and where each acts upstream of a cytokinin-dependent or a cytokinin-independent pathway promoting stem cell specification.

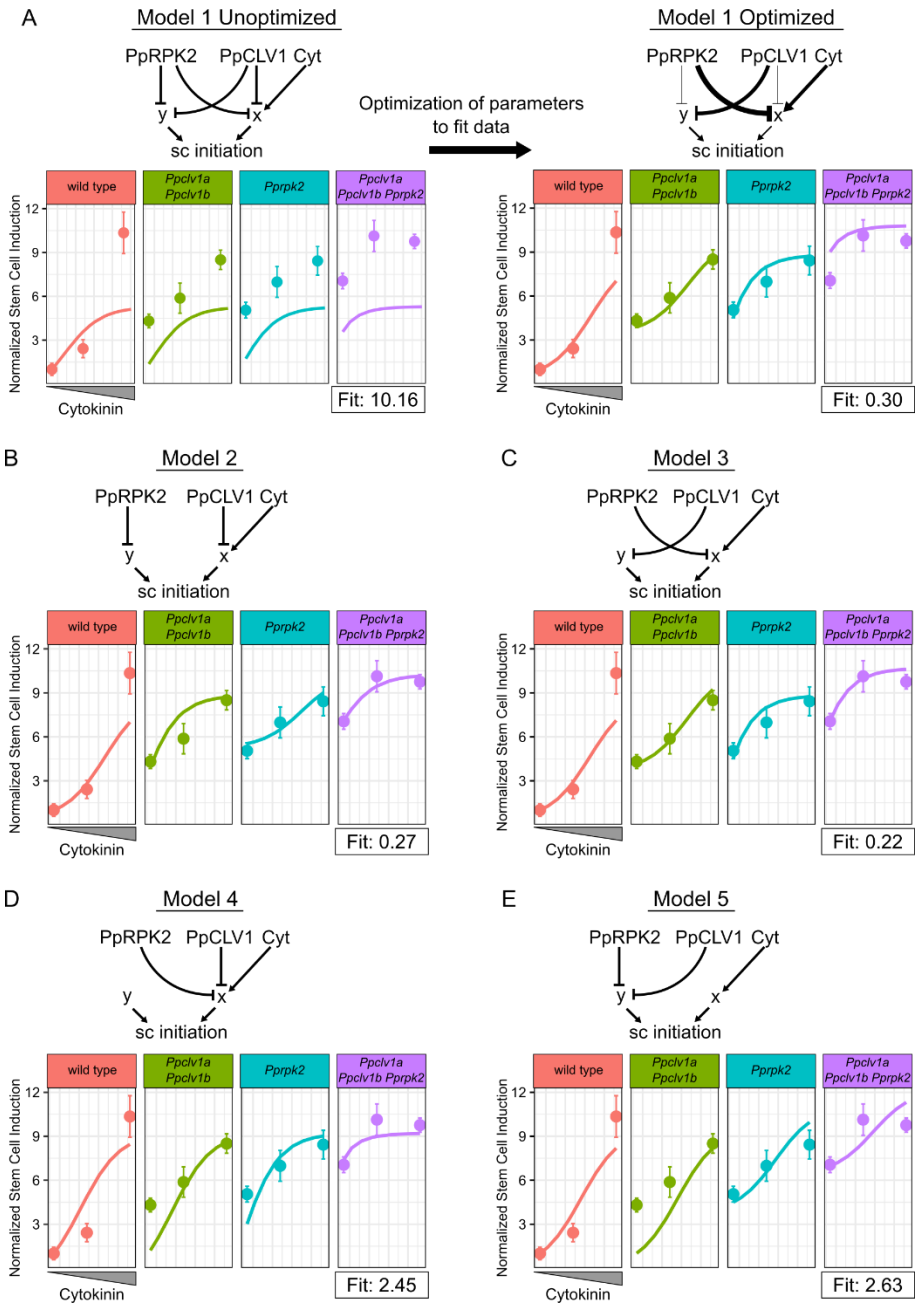

Figure 4: Dynamical model simulations of stem cell production by *Ppclv1a Ppclv1b* and *Pprpk2* mutants over a range of cytokinin concentrations. Basic network depictions and simulation results of mathematical models formalizing five different hypotheses: Model 1 *Pp*CLV1 and *Pp*RPK2 are partially redundant (A); Model 2 *Pp*CLV1 and *Pp*RPK2 are independent with *Pp*CLV1 upstream of cytokinin response (B); Model 3 *Pp*CLV1 and *Pp*RPK2 are independent with *Pp*RPK2 upstream of cytokinin response (C); Model 4 *Pp*CLV1 and *Pp*RPK2 are redundant and upstream of cytokinin response (D); Model 5 *Pp*CLV1 and *Pp*RPK2 are redundant and upstream of a cytokinin-independent pathway (E). On plots, solid lines represent simulated data over a range of cytokinin concentrations. Dots with error bars represent the mean empirical stem cells per μm^2 data and standard errors. From left to right, dots represent values from *P. patens* grown on mock, 10 nM BAP, and 100 nM BAP. In the model on the right side of panel A, the thickness of interaction edges is proportional to the corresponding optimized parameters. Note the empirical data points are based on the data in Figure 3M.

We next compared the extent to which each model could recapitulate the patterns of ectopic stem cell production seen in the empirical data. The behavior and output of a model depends on the parameters selected. Thus, we sought to optimize the parameters in each network to reach the best fit possible to the empirical data. To find the optimal parameters, we coded a random optimizer function (see Supplementaey Methods). Given a network and a set of starting parameters, we used the model to simulate each relevant mutant genotype (wild type, *Ppclv1a Ppclv1b, Pprpk2,* and *Ppclv1a Ppclv1b Pprpk2*) at each level of cytokinin treatment (0 nM BAP, 10 nM BAP, 100 nM BAP). For each model and set of parameters we thus simulated twelve scenarios that we compared with the corresponding mean values from the empirical data. We generated a single fit score that was proportional to the difference between the model and the empirical data (smaller scores indicate a closer fit). Larger differences between simulated and empirical data points were penalized more heavily than smaller ones (See Supplementary Methods). Once a score was generated, each parameter was randomly mutated (adjusted up or down) and a new fit score was calculated and compared to the previous one. If the new fit score was better (lower), the new parameters for that run were adopted as the starting point for the next round of optimization. If the fit score proved worse, the previous parameters were kept as the starting point for the next round of optimization. We ran the optimizer for 300 iterations, allowing the fit score to plateau at a minimum value for each model (see Supplementary Methods).

Using this iterative optimizer, we tested our five competing models of how *Pp*CLV1, *Pp*RPK2, and cytokinin regulate stem cell identity. For model one, the optimizer selected parameters that separated the roles for *Pp*CLV1 and *Pp*RPK2, i.e., the optimizer minimized their redundant activity and emphasized their independent activity (Figure 4 A). Specifically, the optimizer strengthened the regulatory connection between *Pp*RPK2 and cytokinin signaling while weakening the interaction between *Pp*RPK2 and cytokinin-independent stem cell induction, and the optimizer did the opposite for *Pp*CLV1 (Figure 4 A). Thus, the optimized Model 1 was similar to Model 3 (Figure 4 C). Optimized Model 1 reasonably replicated the empirical data with a fit score of 0.3, but notably overestimated the number of ectopic stem cells in the

triple mutant grown in the absence of exogenous cytokinin (Figure 3 A). Models 2 and 3 produced similar fits to Model 1 after optimization with fit scores of 0.27 and 0.22, respectively (Figure 4 B, C). Notably, Model 2 and Model 3 successfully simulated the level of stem cell initiation in triple mutants without exogenous cytokinin. These two models differed from one another predominately in the cytokinin response curves of *Ppclv1a Ppclv1b* and *Pprpk2* mutants (Figure 3 B and C), but neither simulation was far from the empirical data. Finally, Model 4 (fit score = 2.45) and 5 (fit score = 2.63) produced very poor fits to the data (Figure 2 D and E), highlighting the unlikelihood of redundancy between *Pp*CLV1 and *Pp*RPK2. Altogether, the five models support *Pp*CLV1 and *Pp*RPK2 acting through separate pathways. However, the models do not confidently distinguish whether *Pp*CLV1 or *Pp*RPK2 functions upstream of the cytokinin response as either scenario could reproduce the empirical data.

Given that models 2 and 3 best reproduce the empirical data, we used them to predict how stem cell initiation would be affected by the absence of cytokinin signaling (Supplemental figure 4). Each model predicted that, if devoid of cytokinin signaling, each genotype would produce even fewer apical cells. This is consistent with data showing reduced branch stem cell initiation after increasing cytokinin degradation[22]. Informatively, the model predicted that if PpCLV1 functions upstream of cytokinin, blocking cytokinin signaling would suppress the ectopic stem cell phenotype in *Ppclv1a Ppclv1b* double mutants. On the other hand, if PpRPK2 functions upstream of cytokinin, blocking cytokinin signaling would suppress the ectopic stem cell formation in *Pprpk2* mutants (Supplemental Figure 4).

Loss of cytokinin signaling reveals a complex network controlling stem cell specification

Three *PpCYTOKININ HISTIDINE KINASE* (*PpCHK*) genes in *P. patens* encode the known cytokinin receptors, and *chk1 chk2 chk3* triple mutants lack the ability to perceive cytokinin[26,27]. Using CRISPR-Cas9 to mutate *PpCLV1a, PpCLV1b*, and *PpRPK2* in the *Ppchk1 Ppchk2 Ppchk3* background, we generated and confirmed four independent lines of *Ppclv1a Ppclv1b Ppchk1 Ppchk2 Ppchk3* quintuple mutants, two independent *Pprpk2 Ppchk1 Ppchk2 Ppchk3* quadruple mutants, and two *Ppclv1a Ppclv1b Pprpk2 Ppchk1 Ppchk2 Ppchk3* sextuple mutants (Supplemental Figure 5). These higher order mutant filaments and

gametophores were insensitive to growth on BAP, supporting a complete loss of cytokinin perception (Supplemental Figure 6).

Our models predicted that if ectopic stem cell formation in *Ppclv1a Ppclv1b* mutants resulted from increased cytokinin-mediated stem cell initiation, ectopic stem cell formation would be suppressed in the higher order *Ppclv1a Ppclv1b Ppchk1 Ppchk2 Ppchk3* quintuple mutants. Alternatively, if PpRPK2 signaling were upstream of the cytokinin response (x), the *Pprpk2* ectopic stem cell phenotype would be suppressed in *Pprpk2 Ppchk1 Ppchk2 Ppchk3* quadruple mutants. To test our predictions of how loss of cytokinin signaling impacts stem cell specification, we examined gametophores from multiple independent lines of *Ppchk1 Ppchk2 Ppchk3* and higher order mutants at cellular resolution and quantified stem cell abundance (Figure 5, A-E).

Cytokinin induces the formation of gametophores[22] and promotes cell proliferation in phyllids (Figure 3A-C)[28]. Consistent with these functions, the *Ppchk1 Ppchk2 Ppchk3* triple mutants develop gametophores two weeks later than wild-type[27], and once formed, *Ppchk1 Ppchk2 Ppchk3* gametophores produce, slender phyllids with elongated cells in fewer cell files (Figure 5A-D, Supplemental Figure 7). Surprisingly, confocal imaging of *Ppchk1 Ppchk2 Ppchk3* mutant gametophores revealed the formation of ectopic growth axes, indicating increased stem cell production. Higher order *Ppclv1a Ppclv1b Ppchk1 Ppchk2 Ppchk3* quintuple*, Pprpk2 Ppchk1 Ppchk2 Ppchk3* quadruple*,* and *Ppclv1a Ppclv1b Pprpk2 Ppchk1 Ppchk2 Ppchk3* sextuple mutants produced swollen stems with variable degrees of ectopic apical cells (Figure 5 A-E; range of phenotypes illustrated in Supplemental Figure 7; non-normalized data Supplemental Figure 8). We statistically analyzed the full dataset including stem cell quantification from all mutants and genotypes generated thus far using a Poisson Regression. We found that loss of *Pp*CHK function was significantly associated with increased stem cell abundance ($p = 0.013$). Although neither loss of *Pp*CLV1 or *Pp*RPK2 displayed statistically significant interactions with *Pp*CHK loss of function, a negative interaction between *Ppclv1* and *Ppchk* mutations tended towards significance (*clv1:chk* $p = 0.07$; *rpk2:chk* $p = 0.11$), weakly supporting a role for *PpCLV1* upstream of cytokinin. Overall, loss of cytokinin signaling causes ectopic

stem cell formation and does not suppress stem cell initiation, contrary to our predictions. Thus, the *Ppchk1 Ppchk2 Ppchk3* and higher order mutant phenotypes suggest that important features were missing from our dynamical models of stem cell homeostasis.

Incoherent feedforward control of stem cell induction can explain *chk* phenotypes

We hypothesized that the ectopic stem cell phenotype of *Ppchk1 Ppchk2 Ppchk3* triple mutants could be explained by an incoherent feedforward control: in addition to its primary function promoting stem cell formation, cytokinin either (1) represses a pathway that induces stem cell specification, or (2) promotes a pathway that represses stem cell specification. To test the plausibility of these hypotheses, we formalized each as a dynamical model (Model 6 and 7, respectively), each with versions based on Models 2 and 3. For each model, we introduced a factor called z, which is independent of *Pp*CLV1 and *Pp*RPK2 signaling. In Model 6, z induced stem cell initiation and was inhibited by cytokinin (Figure 5 F), while in Model 7 z inhibited stem cell initiation and was itself induced by cytokinin (Figure 5 G). Each model represents an alternative form of the hypothesis that cytokinin promotes stem cell induction but also provides additional input to temper the sensitivity to stem cell specification cues. We predicted that in the complete absence of cytokinin signaling, the loss of this buffering capacity would render stem cell specification hypersensitive to inputs from other pathways, such as those represented by y in the model.

Optimizing each model to the full dataset provides a test of how well each model can capture key trends in the empirical data. Because we previously found that either *Pp*CLV1 *or Pp*RPK2 acted upstream of cytokinin signaling (x), we simulated both scenarios for each model (Figure 5 F, G, Supplemental Figure 9). Model 6 successfully reproduced the trends in the empirical data, and fit better if

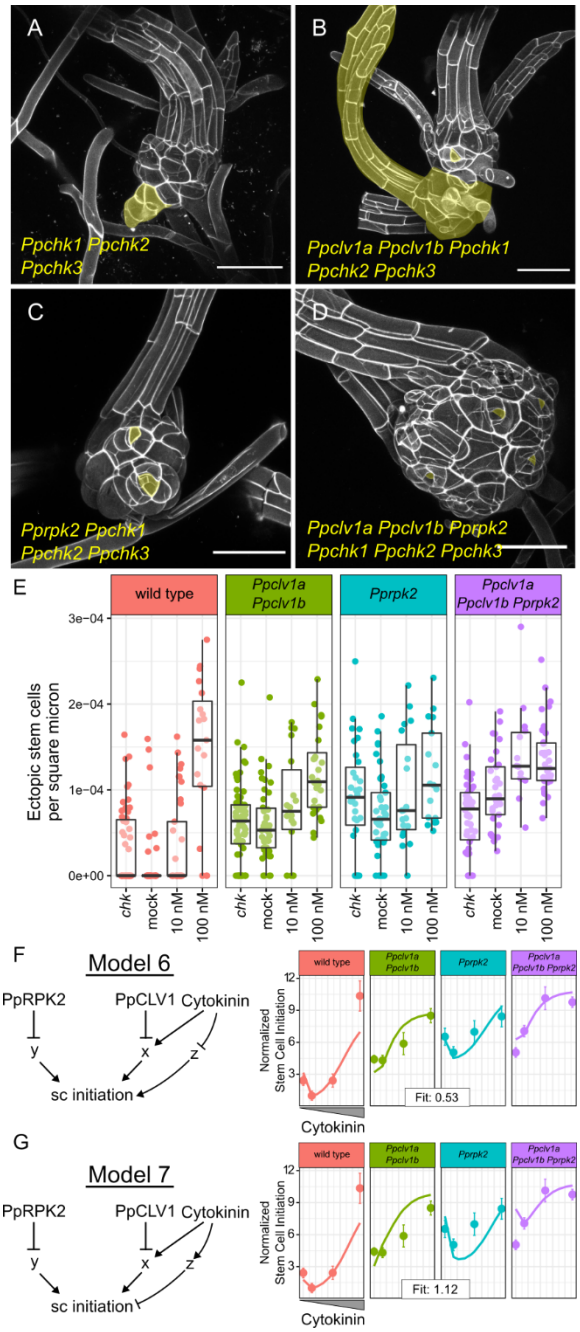

Figure 5: *Ppchk* mutants produce ectopic stem cells and have complex interactions with *Ppclv1* and *Pprpk2* mutants. Gametophores from five week old colonies of *Ppchk* (A), *Ppclv1a Ppclv1b Ppchk1 Ppchk2 Ppchk3* quintuple mutants (B), *Pprpk2 Ppchk1 Ppchk2 Ppchk3* quadruple mutants (C), and *Ppclv1a Ppclv1b Pprpk2 Ppchk1 Ppchk2 Ppchk3* sextuple mutants (D). Ectopic stem cells or derived outgrowths highlighted in yellow. Quantification of ectopic stem cells per μm^2 of visible stem (E), including data from Figure 3M. The range of phenotypes quantified are illustrated in Supplemental Figure 7. Model six posits that cytokinin inhibits an inducer of stem cell identity (F). In model seven, cytokinin promotes an inhibitor of stem cell specification (G). In (F) and (G), solid lines represent simulated data while dots represent mean stem cells per area from the empirical data. Error bars show the standard error. See results section for statistics from Poisson regression.

*Pp*CLV1 were upstream of cytokinin response (fit score = 0.53, Figure 5F) rather than *Pp*RPK2 (fit score = 0.74, Supplemental Figure 9). Model 7 - in which cytokinin induced an independent stem cell inhibitory pathway – fit the data poorly in all cases as it overestimated the number of ectopic stem cells forming in higher order mutants (Model 7 fit scores: 1.12 with and 1.36 with *Pp*CLV1 and *Pp*RPK2 upstream of cytokinin, respectively) (Figure 5 G, Supplemental Figure 8). In comparison, when model 2 and model 3 were fit to this dataset they produced fit scores of 1.85 and 1.59, respectively (Supplemental Figure 10), demonstrating the impact of including 'z' in the model. Overall, a role for cytokinin in buffering stem cell initiation can explain the ectopic stem cell formation in *Ppchk1 Ppchk2 Ppchk3* mutants and higher order *Ppclv1a Ppclv1b Ppchk1 Ppchk2 Ppchk3* and *Pprpk2 Ppchk1 Ppchk2 Ppchk3* mutants.

To test our model that PpCLV1 regulates cytokinin signaling, we used quantitative PCR to measure the expression level of cytokinin-responsive genes as a proxy for broader cytokinin signaling. However, to do so required the validation of bona-fide transcriptional targets of cytokinin signaling in *P. patens*. Looking through an EST dataset measuring transcriptional response to cytokinin in *P. patens*, we found that several *PpCYTOKININ OXIDASE* (*PpCKX*) genes were upregulated in response to cytokinin[29]. Testing the expression of five different *PpCKX* revealed that all were upregulated when colonies were grown on cytokinin, although *PpCKX6* was less sensitive than the others (Supplemental Figure 11A). Thus, the expression levels of *PpCKX* genes might be suitable indicators of transcriptional responses to cytokinin in *P. patens* (Supplemental Figure 11A).

Our best models posit that PpCLV1 represses responses downstream of cytokinin. We thus predicted that, since the expression level of *PpCKX* genes might reflect the level of cytokinin signaling, *PpCKX* expression would be increased in *Ppclv1a Ppclv1b* mutants but unchanged in *Ppclv1a Ppclv1b Ppchk1 Ppchk2 Ppchk3* mutants. Indeed, this pattern was true for the expression of *PpCKX1*, but not for any other CKX genes (Supplemental Figure 11B). While these data provide qualified support for our model, they also indicate the complexity in cytokinin signaling.

One mechanism through which cytokinin might buffer stem cell initiation is by promoting the expression of *PpCLV1a PpCLV1b* or *PpRPK2* genes. qPCR on gametophores grown on mock media revealed variable expression for *PpCLV1a, PpCLV1b,* or *PpRPK2* genes, in agreement with previous promoter GUS fusions[16]. Additionally, no significant increase in *PpCLV1a*, *PpCLV1b*, or *PpRPK2* expression was seen for gametophores grown on 50 nM and 100 nM BAP (Supplemental Figure 11C). Therefore, in accordance with our model, it is unlikely that cytokinin buffers stem cell initiation through the transcriptional regulation of *PpCLV1* or *PpRPK2.*

Discussion

Our work demonstrated similar functions for CLV1 and RPK2 orthologs as regulators of stem cell abundance in the moss *P. patens* as have been previously reported in Arabidopsis. We used a combination of higher-order genetics, hormone treatment, and mathematical modeling to demonstrate that, as in flowering plants, stem-cell identity in *P. patens* gametophores is regulated by interaction between CLV and cytokinin signaling.

*Pp*CLV1 and *Pp*RPK2 signal through distinct pathways

In Arabidopsis, the roles of CLV1 and RPK2 signaling are similar in multiple contexts including stem cell maintenance, carpel development, and anther development[4,21,30,31]. However, depending on the context there is conflicting evidence as to whether CLV1 and its paralogs function in separate or overlapping pathways with RPK2, including evidence for protein-protein interactions between these receptors[4,30–33]. The suite of CLV1 and RPK2-like receptors in *P. patens* is reduced compared to Arabidopsis, making it a powerful system for studying their genetic interactions[16]. *Ppclv1a Ppclv1b* and *Pprpk2* have distinct filament phenotypes, where *Pprpk2* colonies spread faster than wild type or *Ppclv1a Ppclv1b* colonies[34]. This phenotypic distinction could arise from differences in expression patterns, rather than distinct molecular functions. However, *PpCLV1a, PpCLV1b,* and *PpRPK2* are co-expressed in gametophores, where their loss of function render similar mutant phenotypes[16]. Here we show that in *P. patens*, *Pp*CLV1 and *Pp*RPK2 act additively in gametophores, in distinct pathways, to regulate stem-cell specification. In combination with

data in Arabidopsis showing additive effects of *clv1* and *rpk2* mutants in carpel development[4] and the control of gene expression in the SAM[33], these data support a model where in general, CLV1 and RPK2 are not required to act together as a signaling module in plants.

Cytokinin CLV crosstalk has a similar function in *P. patens* and Arabidopsis

In Arabidopsis, CLV1, RPK2, and cytokinin regulate stem-cell identity as part of a network centered around the master regulator gene *WUSCHEL*. In *P. patens*, *PpWOX* genes do not regulate SAM homeostasis[26]. Both exogenous cytokinin and decreased *Pp*CLV1/*Pp*RPK2 function cause similar gametophore phenotypes, including stem swelling and ectopic stem-cell formation. This overlap in phenotypes led us to ask whether *Pp*CLV1/*Pp*RPK2 and cytokinin interact to regulate stem-cell identity in *P. patens*. We tested the response of *Ppclv1a Ppclv1b , Pprpk2,* and *Ppclv1a Ppclv1b Pprpk2* mutants to cytokinin and loss of cytokinin signaling (*Ppchk1 Ppchk2 Ppchk3)* and used mathematical modeling to determine which of seven different hypothetical networks describing *Pp*CLV1, *Pp*RPK2, and cytokinin function could best recapitulate empirical stem-cell specification data. Our data and modeling suggest that either *Pp*CLV1 or *Pp*RPK2 acts upstream of cytokinin-mediated stem-cell induction, with greater support for *Pp*CLV1 performing this role. Our models represent overarching signaling networks, where x and y represent whole signaling cascades, not single genes. Thus, a number of specific molecular networks could fall within the frameworks of the model. Interestingly, this cytokinin-dependent pathway (x in the model, Figure 4, Figure 5) occupies the same position as *WUS* in models describing stem-cell specification in the Arabidopsis SAM[1,35]. This suggests that in the absence of *WUS*, stem-cell abundance is regulated by similar mechanism as described in Arabidopsis, although *WUS* function is replaced by some unknown factor(s).

Cytokinin signaling both induces and inhibits SAM formation

Our analysis of *Ppchk1 Ppchk2 Ppchk3* triple mutants and higher order *Ppclv1a Ppclv1b Ppchk1 Ppchk2 Ppchk3*, *Pprpk2 Ppchk1 Ppchk2 Ppchk3*, and *Ppclv1a Ppclv1b Pprpk2 Ppchk1 Ppchk2 Ppchk3*mutants revealed several unexpected phenotypes. First, we observed that *Ppchk1 Ppchk2 Ppchk3* mutants make ectopic stem cells, contrasting with cytokinin's role promoting stem cell formation. We proposed several

models to explain the counterintuitive *Ppchk1 Ppchk2 Ppchk3* and higher-order mutant phenotypes. An incoherent feedforward model where cytokinin signaling buffers stem cell initiation through a *Pp*CLV1 and *Pp*RPK2-independent pathway successfully replicated the trends seen in the empirical data, over a wide range of mutant genotypes and hormone treatments. However, because little is known about genes promoting SAM formation in *P. patens*, it is difficult to speculate as to the nature of 'z' in the model. It is possible that auxin signaling, which is upstream of stem cell formation on filaments and gametophores, is de-regulated in *Ppchk1 Ppchk2 Ppchk3* mutants[22,36]. However, known stem cell-inducing genes downstream of auxin are not modulated by cytokinin treatment[36,37]. Thus, elucidating the identity of 'z' requires better understanding of cytokinin-responsive genes in gametophores. Recently, *PpRPK2* was shown to modulate auxin homeostasis and transport in protonema[34]. If this interaction holds true in the gametophore, it is also possible that auxin signaling is represented by the 'y' portion of the model.

Common molecular mechanisms can underlie disparate developmental functions across plant evolution

Similarities and differences in stem-cell regulation between the moss *P. patens* and Arabidopsis raise important questions about the evolution of this signaling network. Current phylogenies support a monophyletic clade containing mosses and liverworts, such that mosses and liverworts are equally related to flowering plants. However unlike in *P. patens* and Arabidopsis, CLV1 function in the liverwort *Marchantia polymorpha* enhances stem-cell specification[38]. Interestingly, *MpCLV1*-mediated control of the meristem in Marchantia is also independent of *WOX* genes, supporting the later recruitment of *WOX* genes to regulation of the SAM[38]. Since SAM specification occurs in a *WUS*-independent pathway in bryophytes, is there also a *WUS*-independent pathway in angiosperms? Overall, it is curious how the *P. patens* SAM transcriptome is highly enriched for orthologs of genes that function in angiosperm SAMs, but lacks a role for *WOX* genes, which establish the canonical connection between CLV and cytokinin signaling in flowering plants. These observations raise the question of whether similarities between moss and flowering

plant stem-cell specification pathways are convergent or whether CLV-cytokinin interactions are ancient with *WOX* genes incorporated with the evolution of the multicellular SAM.

P. patens Culture

The Gransden 04 strain of *Physcomitrium patens* (formerly *Physcomitrella patens*) was used for all experiments[39]. To propagate *P. patens*, protonemal tissue was blended in 5-7 ml sterile water using a dremel with a custom propeller blade attachment, and 1-2 ml of moss tissue was inoculated onto BCDAT (see media supplemental table) plates overlain with sterile cellophane. Moss was grown under continuous light at 25°C. For phenotyping gametophores, small samples of freshly blended protonema were placed onto BCD agar media supplemented with the specified amount of filter sterilized BAP. These tufts of tissue grew for the specified time before gametophores were dissected for imaging.

P. patens Transformation

P. patens transformation was conducted as in Whitewoods et al[16,40] but with smaller amounts of tissue (2-4 plates of protonemal tissue) and DNA (10 μg). Smaller transformations were possible due to the efficiency of CRISPR-Cas9 mutagenesis. Transformants were subject to a single round of selection with 20 mg/L G418 in BCDAT plates seven days after transformation.

Plasmid Construction

For routine cloning of gRNAs into a transient expression vector suitable for use in *P. patens*, we used the pENT-U6pro::Bsa1:sgRNA and pENT-U3pro::Bsa1:sgRNA constructs generated previously [16]. To clone gRNA expression vectors, oligonucleotides with overhangs complementary to the BSAI cut sites (GGC and CAT for U3 and U6 promoters, and AAAC to ligate on the 3' end with and were annealed. The annealed oligonucleotides were ligated into pENT-U3pro::Bsa1:sgRNA or pENT-U6pro::Bsa1:sgRNA digested with BSAI. Clones were verified by sequencing. gRNA sequences were selected using the CRISPOR online service[41]. We tried four gRNAs for the *PpCLV1a* gene before finding one that cleaved effectively; the first gRNAs designed for *PpCLV1b* and *PpRPK2* gene successfully induced mutations.

Staining and Imaging

Gametophores were dissected from the periphery of tufts and stained with 5 μg/ml propidium iodide (PI) solution. Imaging was conducted using a Zeiss 710 laser scanning confocal microscope. We used a 514 nm laser for excitation and collected an emission spectrum from 566 to 650 nM. Images were captured using either a 20x water immersion NA 1.0 or 10x lens.

Gametophore Samples

For *Ppclv1* and *Pprpk2* mutant lines, the previously characterized *Ppclv1ab line 6* and *Pprpk2 line a32* were used for all imaging and analysis. For the *Ppclv1a Ppclv1b Pprpk2* triple mutant, *Ppclv1a Ppclv1b Pprpk2 line 3* was used. All data for these lines was collected from tissue grown and imaged on over three separate occasions, with the exception of 10 nM BAP treatments, which were replicated twice. For *Ppchk1 Ppchk2 Ppchk3* and higher order *Ppclv1a Ppclv1b, Pprpk2, and Ppchk* mutants, data represent a mix of CRISPR lines for each genotype grown and imaged on two separate occasions (Supplemental Figure 5D-E).

Ectopic Apical Cell Quantification

Areas of stem visible on maximum intensity projections (not including phyllids) were manually measured using FIJI[42]. These stem measurements were used to account for variability in size and developmental stage across samples. Ectopic apical cells were identified as triangular cells and were distinguished from illusory tetrahedral cells seen in maximum intensity projections by manually looking through z-stacks. Regions of ectopic growth and phyllid production were also counted as ectopic stem cells.

Statistical analysis

Statistical analysis was performed using the R statistical programming language. For regressions, genotypes were coded as a combination of two factors (Ppclv1 and Pprpk2) for the purposes of our analysis, since *Ppclv1a* and *Ppclv1b* single mutants were not analyzed separately. The effects of mutating *PpCLV1* and *PpRPK2* and of growth on 10 nM and 100 nM BAP as well as the interactions between these three factors (*PpCLV1*, *PpRPK2*, and the exogenous cytokinin) were modeled using a Poisson general linear model that included stem area as an offset (model: glm(total_ectopic ~ clv1 + rpk2 + exock + clv1L:rpk2L + clv1L:exock + rpk2L:exock + (log(area)), family = 'poisson'). BAP concentrations were treated as a continuous variable with levels of zero, ten, and one hundred.

qPCR

RNA was extracted from gameotophores using the Qiagen plant RNeasy mini kit, followed by reverse transcription with SuperScript® III First-Strand Synthesis System for RT-PCR. Reactions were run in a Roche Lightcycler 480 with three biological and three technical replicates for each sample. 60s ribosomal RNA was used as a reference, and data was analyzed using the delta delta cp method[43].

Acknowledgements

We would like to thank the Cornell Statistical Consulting unit and Celine Cammarata for advice on statistical analyses and data processing. We thank Klaus von Schwartzenberg for sharing the *cytokinin*

histidine kinase triple mutant lines. We also thank Jill Harrison and Zoe Nemec Venza for thoughtful and helpful discussions about this work. We finally would like to acknowledge Jill Harrison, Zoe Nemec Venza, Mingyuan Zhu, Kate Harline, and Shuyao Kong for comments on the manuscript. This research was supported by NSF IOS-1238142 to M.J.S. and NSF IOS-1553030 to A.H.K.R., the Schmittau-Novak Small Grant to J.C., the Cornell Provost Diversity Dissertation Completion Fellowship to J.C., funding from the Weill Institute for Cell and Molecular Biology to A.H.K.R., and the NSF funded Boyce Thompson Institute Cornell REU program support for C.M.F (REU #1850796).

References

1. Brand, U., Fletcher, J.C., Hobe, M., Meyerowitz, E.M., and Simon, R. (2000). Dependence of Stem Cell Fate in Arabidopsis on a Feedback Loop Regulated by CLV3 Activity. Science (80-.). *289*, 617–619.

2. Fletcher, J.C., Brand, U., Running, M.P., Simon, R., and Meyerowitz, E.M. (1999). Signaling of cell fate decisions by CLAVATA3 in Arabidopsis shoot meristems. Science *283*, 1911–1914.

3. Rojo, E., Sharma, V.K., Kovaleva, V., Raikhel, N. V, and Fletcher, J.C. (2002). CLV3 is localized to the extracellular space, where it activates the Arabidopsis CLAVATA stem cell signaling pathway. Plant Cell *14*, 969–977.

4. Kinoshita, A., Betsuyaku, S., Osakabe, Y., Mizuno, S., Nagawa, S., Stahl, Y., Simon, R., Yamaguchi-Shinozaki, K., Fukuda, H., and Sawa, S. (2010). RPK2 is an essential receptor-like kinase that transmits the CLV3 signal in Arabidopsis. Development *137*, 3911–3920.

5. Kayes, J.M., and Clark, S.E. (1998). CLAVATA2, a regulator of meristem and organ development in Arabidopsis. Development *125*, 3843–3851.

6. Clark, S.E., Running, M.P., and Meyerowitz, E.M. (1995). CLAVATA3 is a specific regulator of shoot and floral meristem development affecting the same processes as CLAVATA1. Development *121*.

7. Riedel-Kruse, I.H., Müller, C., and Oates, A.C. (2007). Synchrony dynamics during initiation, failure, and rescue of the segmentation clock. Science *317*, 1911–1915.

8. Müller, R., Bleckmann, A., and Simon, R. (2008). The receptor kinase CORYNE of Arabidopsis transmits the stem cell-limiting signal CLAVATA3 independently of CLAVATA1. Plant Cell *20*, 934–946.

9. Yadav, R.K., Perales, M., Gruel, J., Girke, T., Jönsson, H., and Venugopala Reddy, G. (2011). WUSCHEL protein movement mediates stem cell homeostasis in the Arabidopsis shoot apex. Genes Dev. *25*, 2025–2030.

10. Daum, G., Medzihradszky, A., Suzaki, T., and Lohmann, J.U. (2014). A mechanistic framework for noncell autonomous stem cell induction in Arabidopsis. Proc. Natl. Acad. Sci. *111*, 14619–14624.

11. Laux, T., Mayer, K.F.X., Berger, J., and Jürgens, G. (1996). The WUSCHEL gene is required for

shoot and floral meristem integrity in Arabidopsis. Development *122*, 87–96.

12. Mayer, K.F.X., Schoof, H., Haecker, A., Lenhard, M., Jürgens, G., and Laux, T. (1998). Role of WUSCHEL in Regulating Stem Cell Fate in the Arabidopsis Shoot Meristem. Cell *95*, 805–815.

13. Harrison, C.J., Roeder, A.H.K., Meyerowitz, E.M., and Langdale, J. a. (2009). Local Cues and Asymmetric Cell Divisions Underpin Body Plan Transitions in the Moss Physcomitrella patens. Curr. Biol. *19*, 461–471.

14. Frank, M.H., and Scanlon, M.J. (2014). Transcriptomic Evidence for the Evolution of Shoot Meristem Function in Sporophyte-Dominant Land Plants through Concerted Selection of Ancestral Gametophytic and Sporophytic Genetic Programs. Mol. Biol. Evol. *32*, 355–367.

15. Cammarata, J., and Scanlon, M.J. (2020). A functionally informed evolutionary framework for the study of LRR-RLKs during stem cell maintenance. J. Plant Res. *133*, 331–342.

16. Whitewoods, C.D., Cammarata, J., Nemec Venza, Z., Sang, S., Crook, A.D., Aoyama, T., Wang, X.Y., Waller, M., Kamisugi, Y., Cuming, A.C., et al. (2018). CLAVATA Was a Genetic Novelty for the Morphological Innovation of 3D Growth in Land Plants. Curr. Biol. *28*, 1–12.

17. Nardmann, J., and Werr, W. (2012). The invention of WUS-like stem cell-promoting functions in plants predates leptosporangiate ferns. Plant Mol. Biol. *78*, 123–134.

18. Ikeda, M., Mitsuda, N., and Ohme-Takagi, M. (2009). Arabidopsis wuschel is a bifunctional transcription factor that acts as a repressor in stem cell regulation and as an activator in floral patterning. Plant Cell *21*, 3493–3505.

19. Lin, H., Niu, L., McHale, N. a, Ohme-Takagi, M., Mysore, K.S., and Tadege, M. (2013). Evolutionarily conserved repressive activity of WOX proteins mediates leaf blade outgrowth and floral organ development in plants. Proc. Natl. Acad. Sci. U. S. A. *110*, 366–71.

20. Sakakibara, K., Reisewitz, P., Aoyama, T., Friedrich, T., Ando, S., Sato, Y., Tamada, Y., Nishiyama, T., Hiwatashi, Y., Kurata, T., et al. (2014). WOX13-like genes are required for reprogramming of leaf and protoplast cells into stem cells in the moss Physcomitrella patens. Development *141*, 1660–1670.

21. Cammarata, J., Roeder, A.H., and Scanlon, M.J. (2019). Cytokinin and CLE signaling are highly intertwined developmental regulators across tissues and species. Curr. Opin. Plant Biol. *51*, 96–104.

22. Coudert, Y., Palubicki, W., Ljung, K., Novak, O., Leyser, O., and Harrison, C.J. (2015). Three ancient hormonal cues co-ordinate shoot branching in a moss. Elife, 1–26.

23. Meng, W.J., Cheng, Z.J., Sang, Y.L., Zhang, M.M., Rong, X.F., Wang, Z.W., Tang, Y.Y., and Zhang, X.S. (2017). Type-B ARABIDOPSIS RESPONSE REGULATORs Is Critical to the Specification of Shoot Stem Cell Niche by Dual Regulation of WUSCHEL. Plant Cell *29*, tpc.00640.2016.

24. Gordon, S.P., Heisler, M.G., Reddy, G. V., Ohno, C., Das, P., and Meyerowitz, E.M. (2007). Pattern formation during de novo assembly of the Arabidopsis shoot meristem. Development *134*, 3539–3548.

25. Clark, S.E., Williams, R.W., and Meyerowitz, E.M. (1997). The CLAVATA1 gene encodes a putative receptor kinase that controls shoot and floral meristem size in Arabidopsis. Cell *89*, 575–585.

26. Ishida, K., Yamashino, T., Nakanishi, H., and Mizuno, T. (2010). Classification of the genes involved in the two-component system of the moss Physcomitrella patens. Biosci. Biotechnol. Biochem. *74*, 2542–2545.

27. von Schwartzenberg, K., Lindner, A., Gruhn, N., Šimura, J., Novák, O., Strnad, M., Gonneau, M., Nogué, F., Heyl, A., Schwartzenberg, K. Von, et al. (2015). CHASE domain-containing receptors play an essential role in the cytokinin response of the moss Physcomitrella patens. J. Exp. Bot. *67*, 667–679.

28. Barker, E.I., and Ashton, N.W. (2013). Heteroblasty in the moss, *Aphanoregma patens* (*Physcomitrella patens*), results from progressive modulation of a single fundamental leaf developmental programme. J. Bryol. *35*, 185–196.

29. Nishiyama, T., Fujita, T., Shin-i, T., Seki, M., Nishide, H., Uchiyama, I., Kamiya, A., Carninci, P., Hayashizaki, Y., Shinozaki, K., et al. (2003). Comparative genomics of Physcomitrella patens gametophytic transcriptome and Arabidopsis thaliana : Implication for land plant evolution. PNAS *100*, 8007–8012.

30. Hord, C.L.H., Chen, C., DeYoung, B.J., Clark, S.E., and Ma, H. (2006). The BAM1/BAM2 receptor-like kinases are important regulators of Arabidopsis early anther development. Plant Cell *18*, 1667–80.

31. Cui, Y., Hu, C., Zhu, Y., Cheng, K., Li, X., Wei, Z., Xue, L., Lin, F., Shi, H., Yi, J., et al. (2018). CIK Receptor Kinases Determine Cell Fate Specification during Early Anther Development in Arabidopsis. Plant Cell *30*, 2383–2401.

32. Shimizu, N., Ishida, T., Yamada, M., Shigenobu, S., Tabata, R., Kinoshita, A., Yamaguchi, K., Hasebe, M., Mitsumasu, K., and Sawa, S. (2015). BAM 1 and RECEPTOR-LIKE PROTEIN KINASE 2 constitute a signaling pathway and modulate CLE peptide-triggered growth inhibition in Arabidopsis root. New Phytol. *3*, 1104–1113.

33. Nimchuk, Z.L. (2017). CLAVATA1 controls distinct signaling outputs that buffer shoot stem cell proliferation through a two-step transcriptional compensation loop. PLoS Genet. *13*.

34. Nemec-Venza, Z., Madden, C., Stewart, A., Liu, W., Novák, O., Pěnčík, A., Cuming, A.C., Kamisugi, Y., and Harrison, C.J. (2022). *CLAVATA* modulates auxin homeostasis and transport to regulate stem cell identity and plant shape in a moss. New Phytol.

35. Gordon, S.P., Chickarmane, V.S., Ohno, C., and Meyerowitz, E.M. (2009). Multiple feedback loops through cytokinin signaling control stem cell number within the Arabidopsis shoot meristem. Proc. Natl. Acad. Sci. U. S. A. *106*, 16529–16534.

36. Aoyama, T., Hiwatashi, Y., Shigyo, M., Kofuji, R., Kubo, M., Ito, M., and Hasebe, M. (2012). AP2-type transcription factors determine stem cell identity in the moss Physcomitrella patens. Development *139*, 3120–3129.

37. Moody, L.A., Kelly, S., Rabbinowitsch, E., Langdale, J.A., Moody, L.A., Kelly, S., Rabbinowitsch, E., and Langdale, J.A. (2018). Genetic Regulation of the 2D to 3D Growth Transition in the Moss Physcomitrella patens Report Genetic Regulation of the 2D to 3D Growth Transition in the Moss Physcomitrella patens. Curr. Biol. *28*, 1–6.

38. Hirakawa, Y., Fujimoto, T., Ishida, S., Uchida, N., Sawa, S., Kiyosue, T., Ishizaki, K., Nishihama, R., Kohchi, T., and Bowman, J.L. (2020). Induction of Multichotomous Branching by CLAVATA Peptide

in Marchantia polymorpha. Curr. Biol. *30*, 3833-3840.e4.

39. Ashton, N.W., and Cove, D.J. (1977). The isolation and preliminary characterisation of auxotrophic and analogue resistant mutants of the moss, Physcomitrella patens. MGG Mol. Gen. Genet.

40. Schaefer, D., Zryd, J.-P., Knight, C.D., and Cove, D.J. (1991). Stable transformation of the moss Physcomitrella patens. Mol. Gen. Genet., 418–424.

41. Haeussler, M., Schönig, K., Eckert, H., Eschstruth, A., Mianné, J., Renaud, J.B., Schneider-Maunoury, S., Shkumatava, A., Teboul, L., Kent, J., et al. (2016). Evaluation of off-target and on-target scoring algorithms and integration into the guide RNA selection tool CRISPOR. Genome Biol. *17*, 1–12.

42. Schindelin, J., Arganda-Carreras, I., Frise, E., Kaynig, V., Longair, M., Pietzsch, T., Preibisch, S., Rueden, C., Saalfeld, S., Schmid, B., et al. (2012). Fiji: An open-source platform for biological-image analysis. Nat. Methods.

43. Livak, K.J., and Schmittgen, T.D. (2001). Analysis of relative gene expression data using real-time quantitative PCR and the 2-ΔΔCT method. Methods *25*, 402–408.

Supplemental Figures

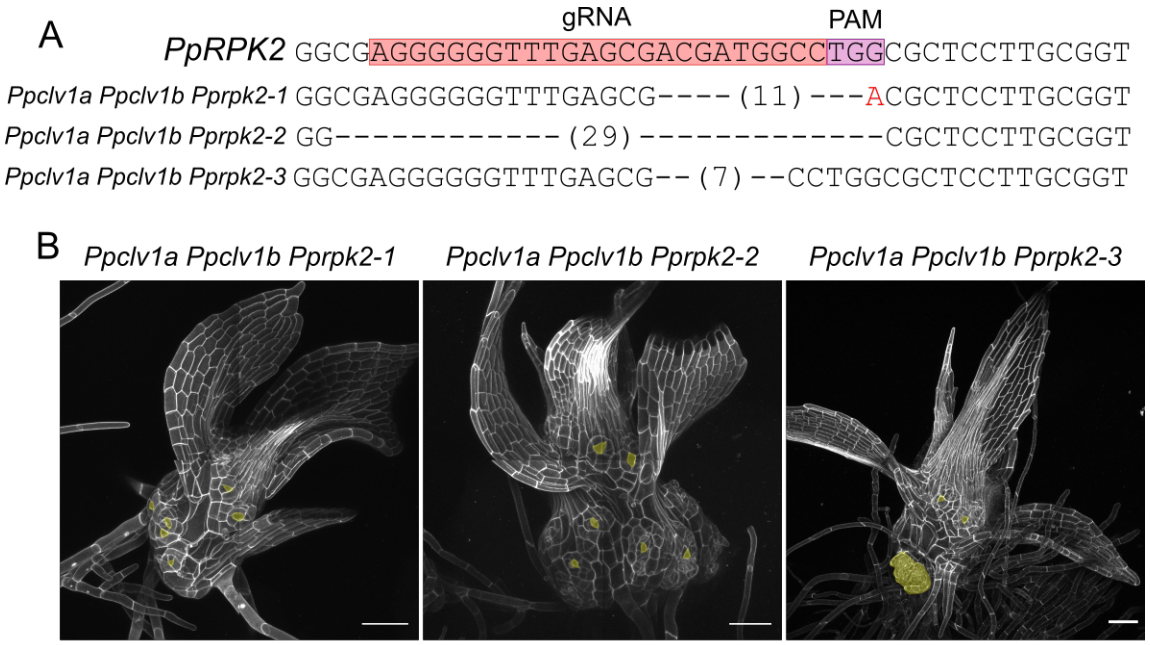

Supplemental Figure 1: Characterization of three *Ppclv1a Ppclv1b Pprpk2* triple mutant lines. We transformed *Ppclv1a Ppclv1b-8* double mutants (Whitewoods, Cammarata et al. 2018) with plasmids expressing a *PpRPK2*-targeting gRNA, Cas9, and a selectable marker. We generated independent lines with *Pprpk2*-like colony phenotypes and selected three for in-depth phenotyping of gametophore morphogenesis, shown here. **A)** Portion of *PpRPK2* exon 1 with gRNA target sequence and PAM (Protospacer Adjacent Motif) highlighted. Below, aligned sequences of the *Pprpk2* mutant loci from three *Ppclv1 Pprpk2* lines. **B)** All *Ppclv1 Pprpk2* mutants display the short stature, ectopic stem cell phenotypes, and ectopic midrib specification representative of a combination of *Ppclv1* and *Pprpk2* phenotypes.

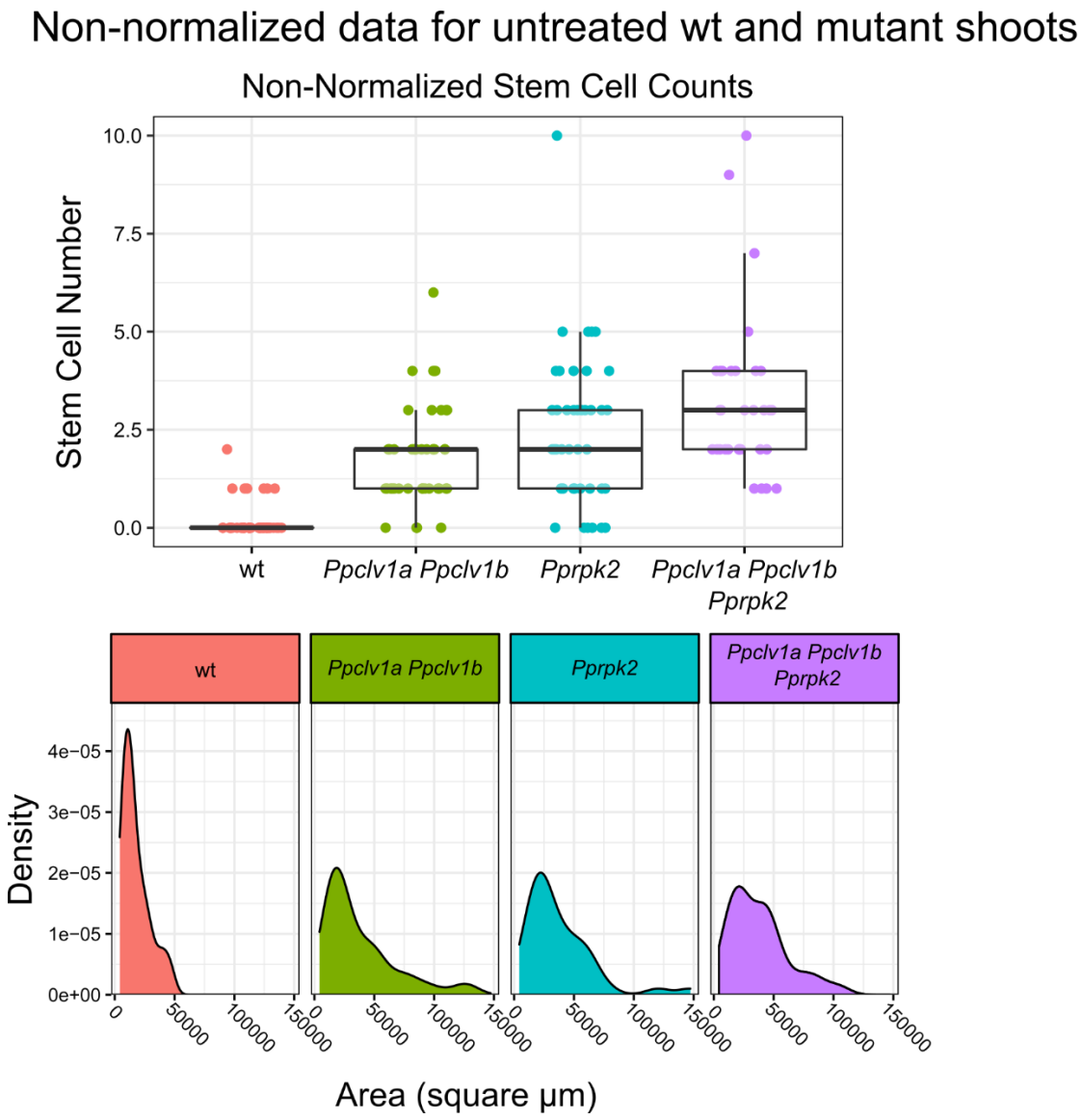

Supplemental Figure 2: Non-normalized data set of wt, *Ppclv1a Ppclv1b*, *Pprpk2*, and *Ppclv1a Ppclv1b Pprpk2* gametophores. Top panel: boxplot representing raw number of stem cells observed on gametophores at each condition. Lower panel: density plot showing distribution of stem areas from which stem cell measurements were taken.

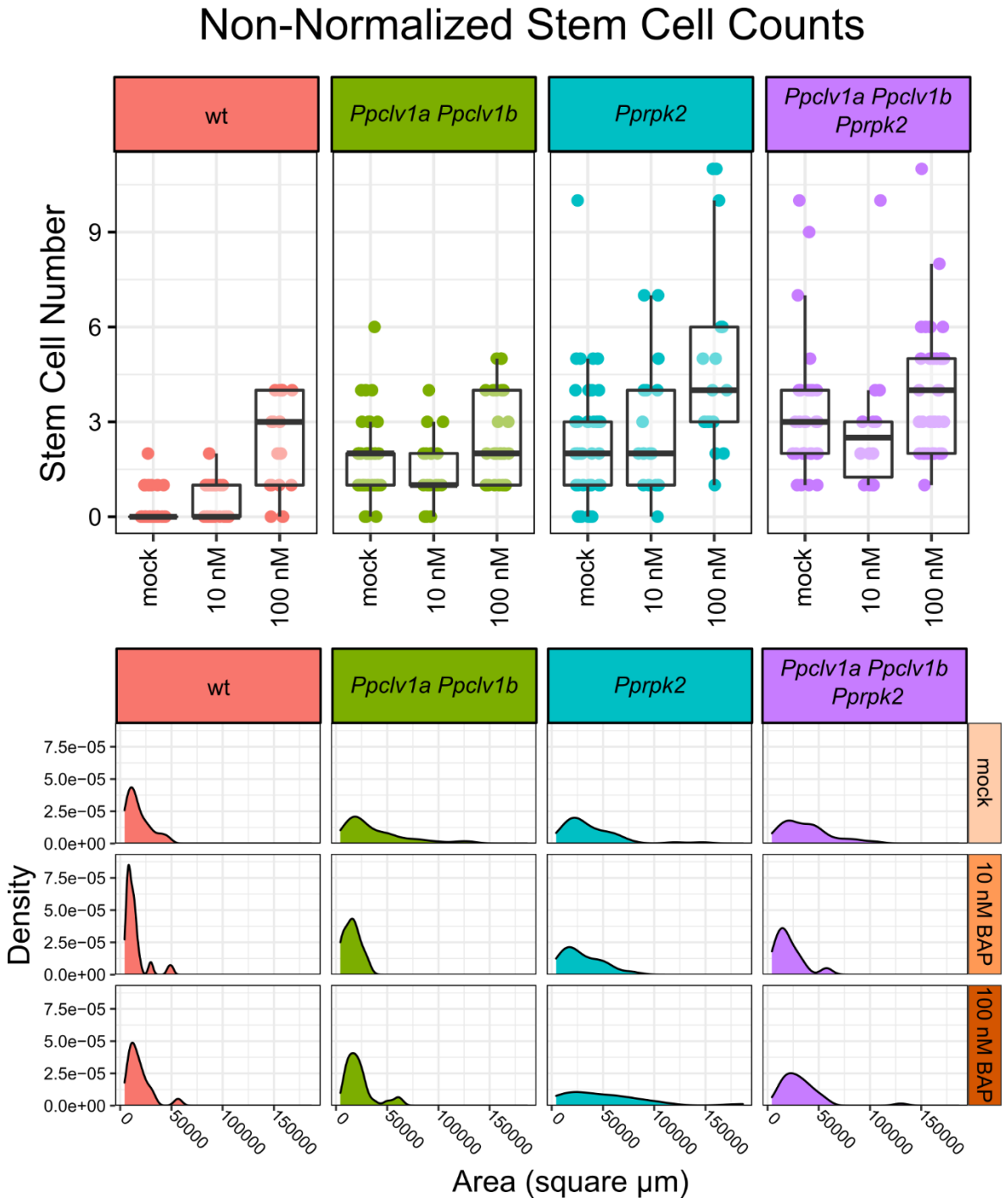

Supplemental Figure 3: Non-normalized data set of mock and cytokinin-treated wt, *Ppclv1a Ppclv1b*, *Pprpk2*, and *Ppclv1a Ppclv1b Pprpk2* gametophores. Top panel: boxplot representing raw number of stem cells observed on gametophores at each condition. The normalized data is presented in Figure 3M. Lower panel: density plot showing distribution of stem areas from which stem cell measurements were taken. Includes data from Supplemental Figure 2 to parallel main text. See results section for statistics from Poisson regression.

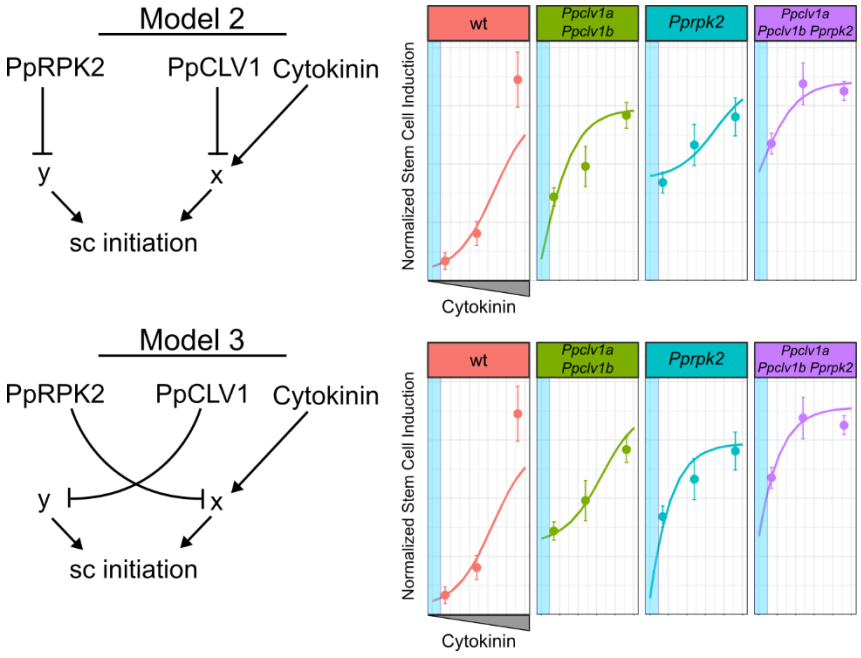

Supplemental Figure 4: Predictions of stem cell initiation at zero cytokinin. The best performing models of stem cell initiation in wild type *Ppclv1a Ppclv1b*, *Pprpk2*, and *Ppclv1a Ppclv1b Pprpk2* triple mutants with and without exogenous cytokinin were used to predict stem cell initiation levels if cytokinin signaling were abolished (highlighted blue). Each model predicted a reduction in stem cell initiation. More informatively, mutants of whichever gene that acts upstream of *x* would see their stem cell initiation phenotypes fully suppressed upon reduced cytokinin (*PpRPK2* above, *PpCLV1* below). Data points and error bars represent empirical stem cell per area values normalized to wild type grown on mock-treated media. From left to right: mock, 10 nM BAP, 100 nM BAP. Solid lines represent model simulations after optimization of parameters to the data.

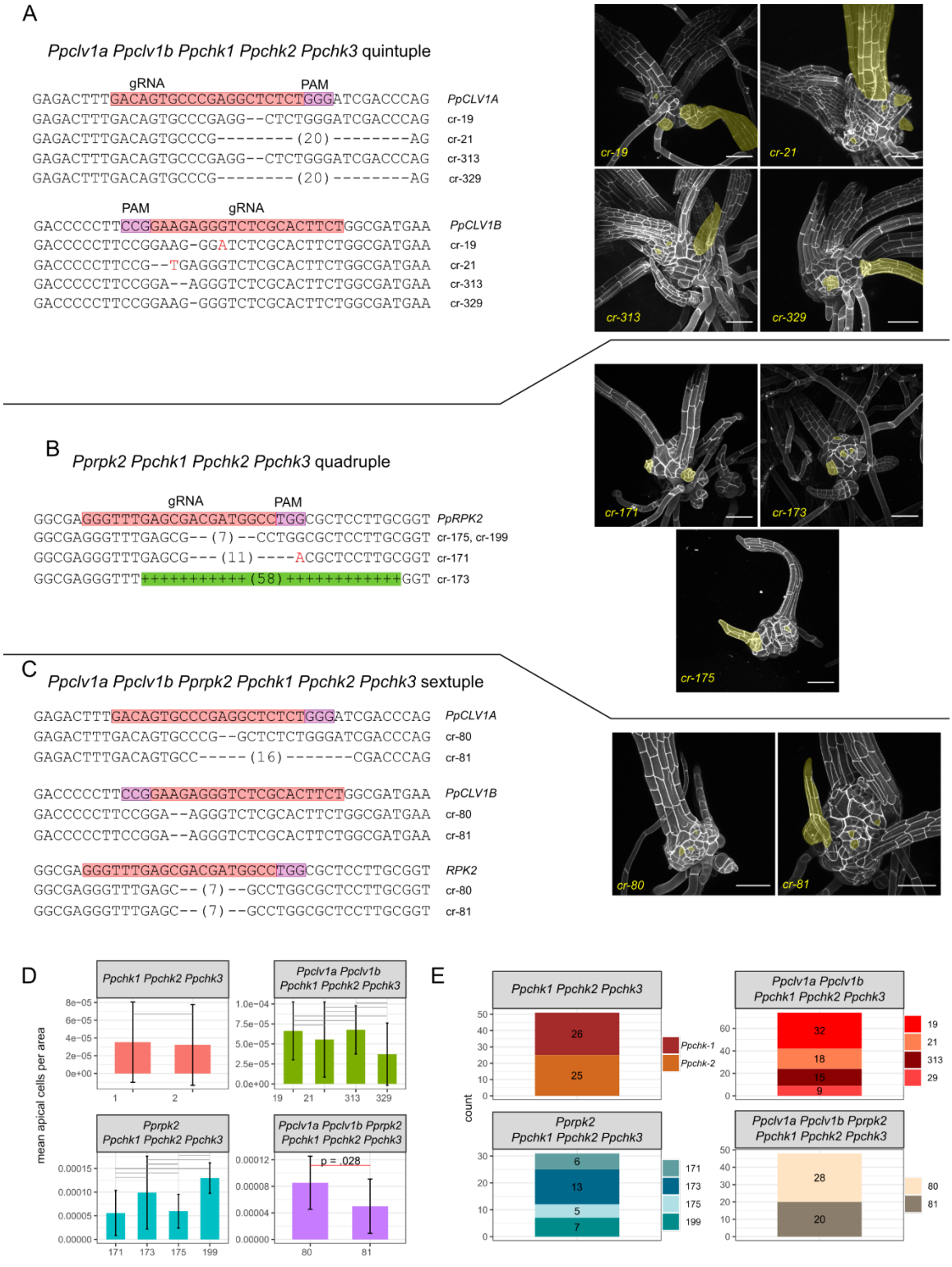

Supplemental Figure 5: genotyping higher order *Ppclv1 Pprpk2 Ppchk* mutants. *Ppchk1 Ppchk2 Ppchk3-1* plants were transformed with gRNAs targeting *PpCLV1a* and *PpCLV1b*, *PpRPK2*, or all three. Three independent lines for *Ppclv1a Ppclv1b Ppchk1 Ppchk2 Ppchk3* quintuple mutants (A) and *Pprpk2 Ppchk1 Ppchk2 Ppchk3* quadruple mutants were obtained (B). A *Ppclv1b Pprpk2 Ppchk1 Ppchk2*

Ppchk3 quintuple mutant line was recovered and re-transformed with a *PpCLV1a*-targeting gRNA to generate two sextuple mutant lines (C). CRISPR mutant lines are indicated with *cr-#*. On the right, examples of gametophore phenotypes for each of these lines show a combination of *Ppclv1, Pprpk2*, and *Ppchk* phenotypes. Comparison of stem cell phenotype across mutant lines, with pairwise tests showing that no lines are significantly different from any other of the same genotype except for *cr-80* and *cr-81* (D). Non-significant results (Bonferroni correction-adjusted $p > 0.05$) are represented by gray lines; significant results in red. Distribution of lines used to generate the data for each genotype (E).

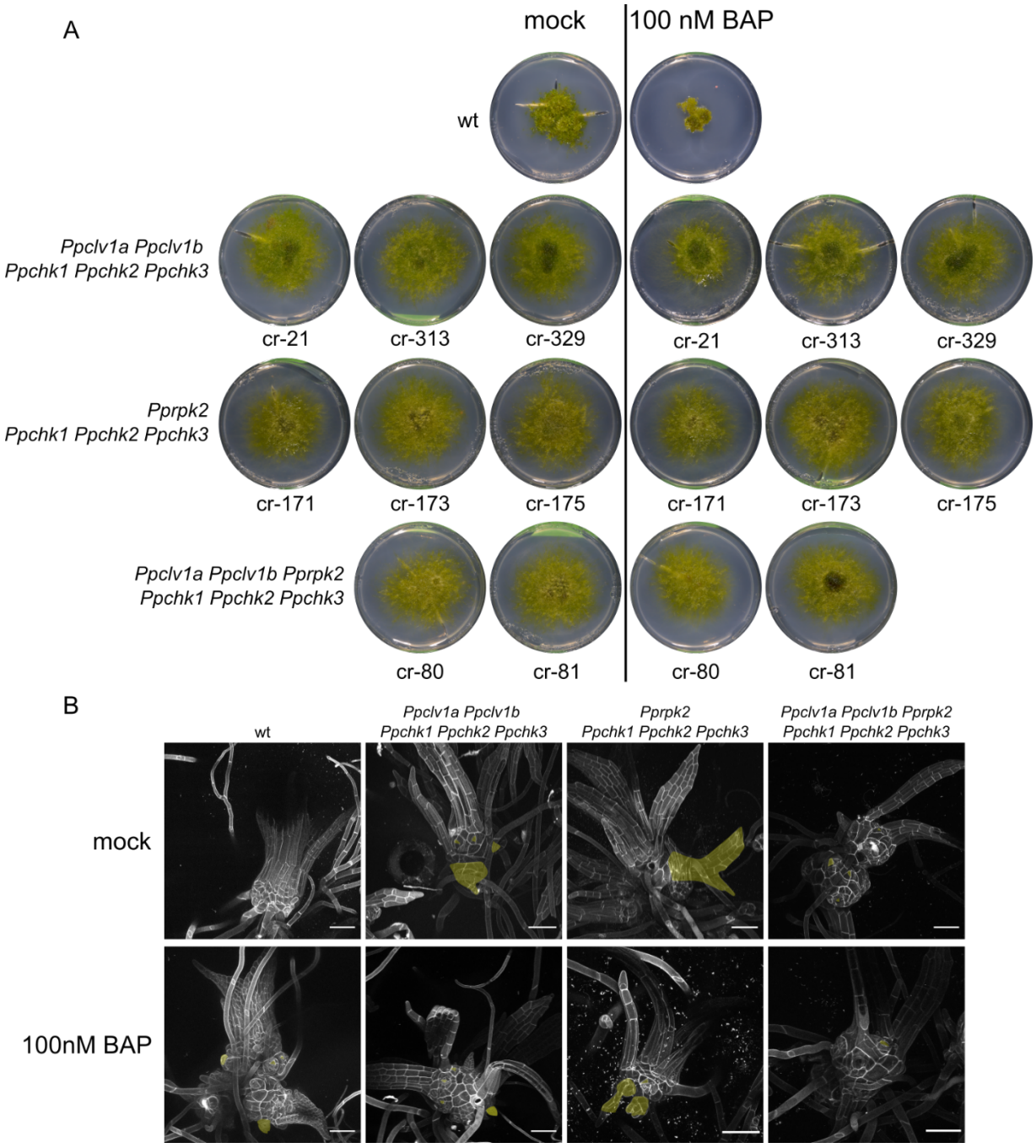

Supplemental Figure 6: *Ppchk* mutants are insensitive to cytokinin. A) Five week-old *P. patens* tufts grown on mock (left) or 100 nM BAP (right). From top to bottom, wild type, *Ppclv1a Ppclv1b Ppchk1 Ppchk2 Ppchk3, Pprpk2 Ppchk1 Ppchk2 Ppchk3*, and *Ppclv1a Ppclv1b Pprpk2 Ppchk1 Ppchk2 Ppchk3* mutants with independent mutant lines tested. B) Confocal images of gametophores from colonies in panel A. Wild type *P. patens* responds to 100 nM BAP whereas *Ppchk1 Ppchk2 Ppchk3* mutant lines do not.

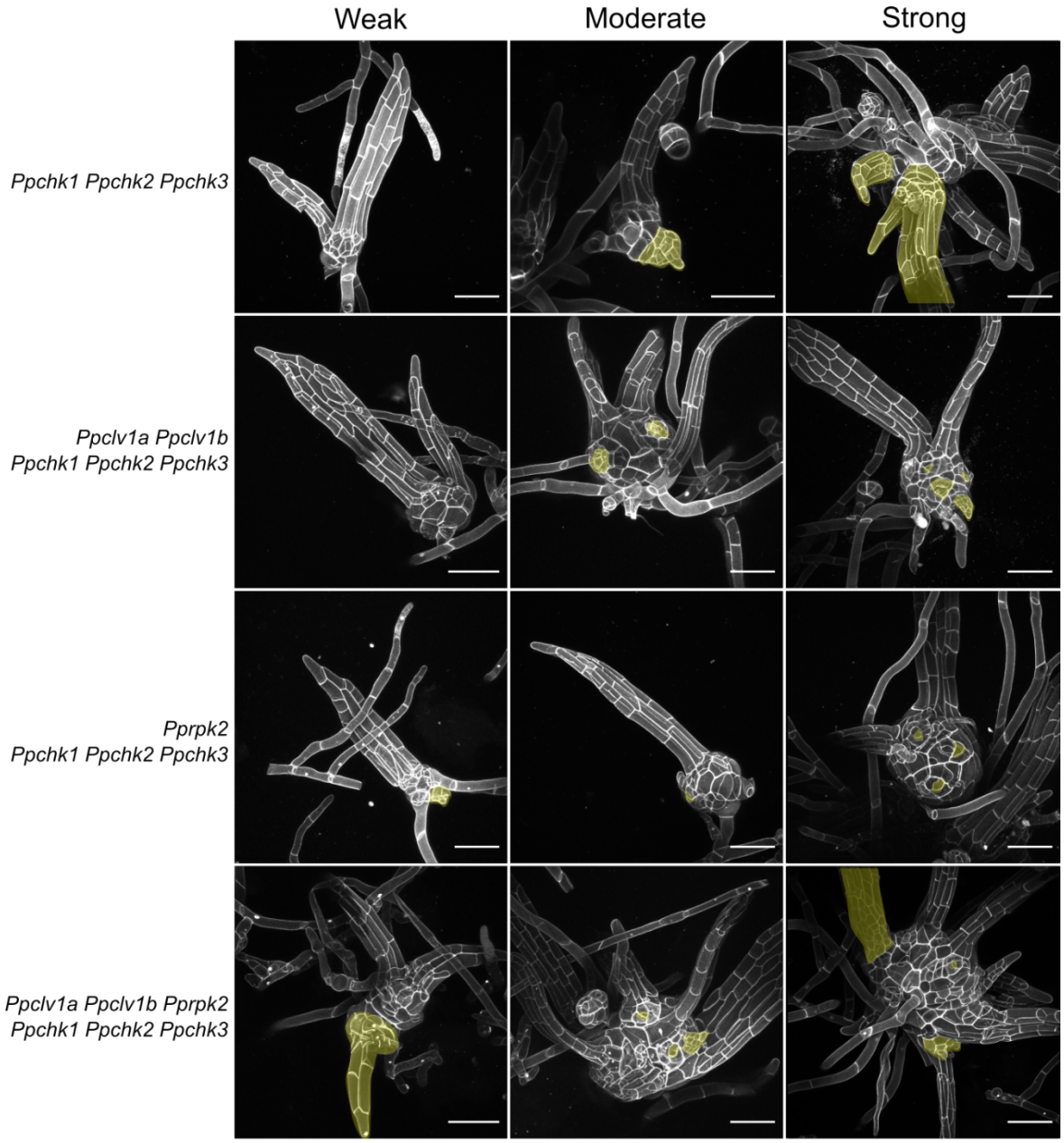

Supplemental Figure 7: Higher order *Ppclv1, Pprpk2,* and *Ppchk* mutant phenotypes are variable. Examples of weak, moderate, and strong phenotypes observed for *Ppchk* mutant gametophores and each higher order *Ppclv1 Ppchk, Pprpk2 Ppchk*, and *Ppclv1 Pprpk2 Ppchk* mutants. *Pprpk2 Ppchk1 Ppchk2 Ppchk3* quadruple mutant phenotypes were particularly variable. However, when quantified these lines still presented an increased initiation of stem cells per area (Figure 5 E).

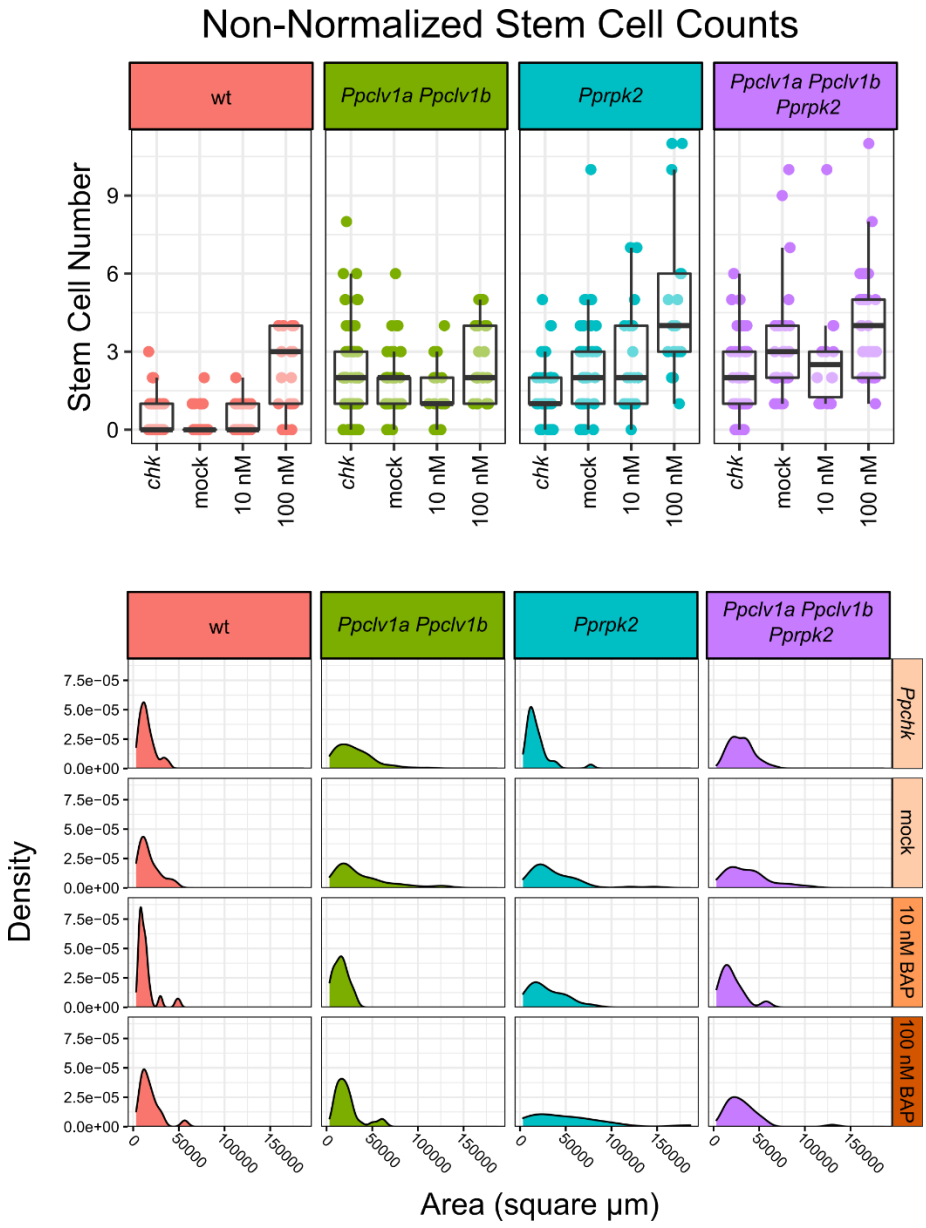

Supplemental Figure 8: Full non-normalized data set. Top panel: boxplot representing raw number of stem cells observed on gametophores at each condition. The normalized data is presented in Figure 5E. Lower panel: density plot showing distribution of stem areas from which stem cell measurements were taken. Here are the data for all gametophores measured across genotypes and treatment conditions. Includes data from supplemental figure 3 to parallel main text. See results section for statistics from Poisson regression.

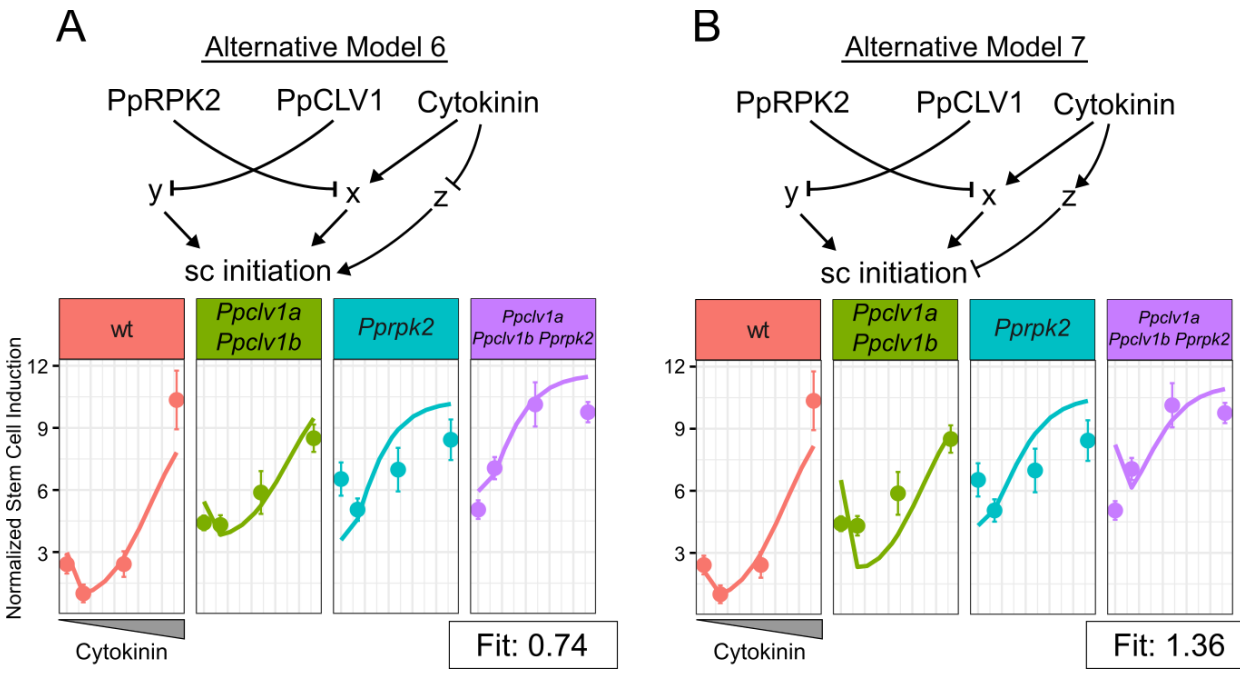

Supplemental Figure 9: Models fit poorly with *PpRPK2* upstream of cytokinin response. Alternative versions of models 6 and 7 (Figure 5), with *PpRPK2* upstream of cytokinin-mediated stem cell induction (x). To Solid lines represent simulated data while dots represent mean stem cells per area from the empirical data. Error bars show the standard error. The x axis shows a log transformation of the cytokinin value input to the model.

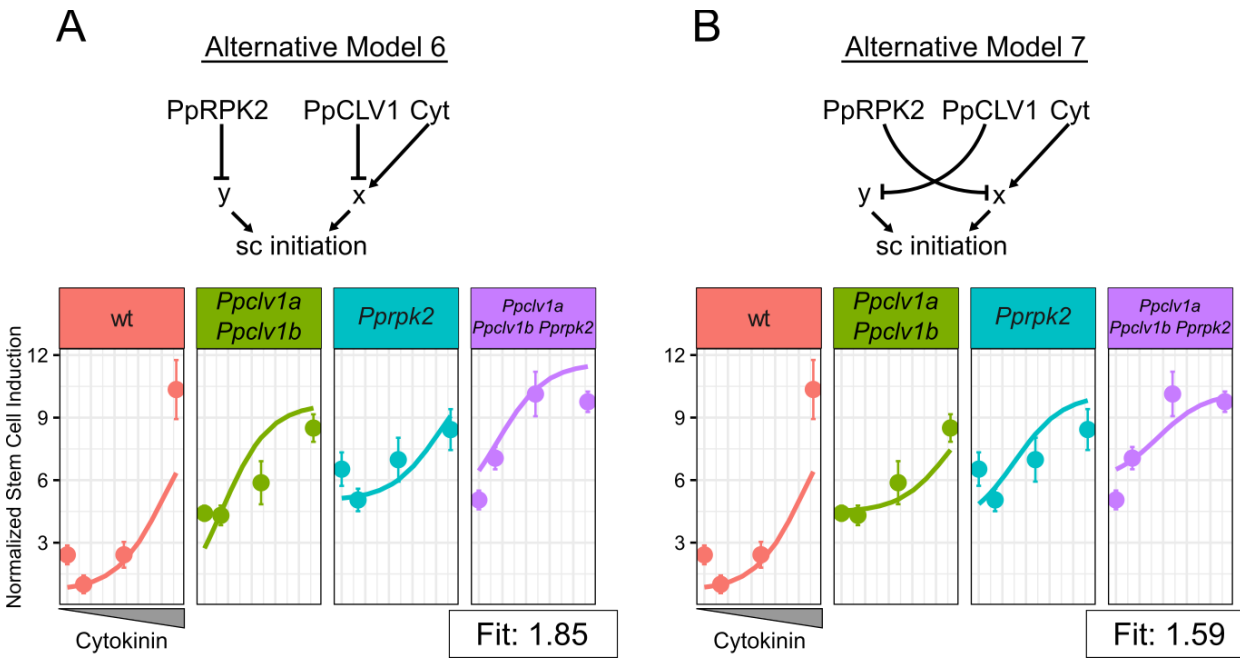

Supplemental Figure 10: Models lacking incoherent feed-forward control cannot recapitulate *Ppchk* and higher order *Ppclv Pprpk2 Ppchk* phenotypes. The models that best fit the stem cell phenotypes of wt, *Ppclv1a Ppclv1b*, *Pprpk2*, and *Ppclv1a Ppclv1b Pprpk2* gametophores on mock and cytokinin treatments were fit to the full dataset including the *Ppchk1 Ppchk2 Ppchk3* and higher order *Ppclv1, Pprpk2, Ppchk* mutants (leftmost datapoint on each plot). Dots represent empirical data; lines represent simulated data.

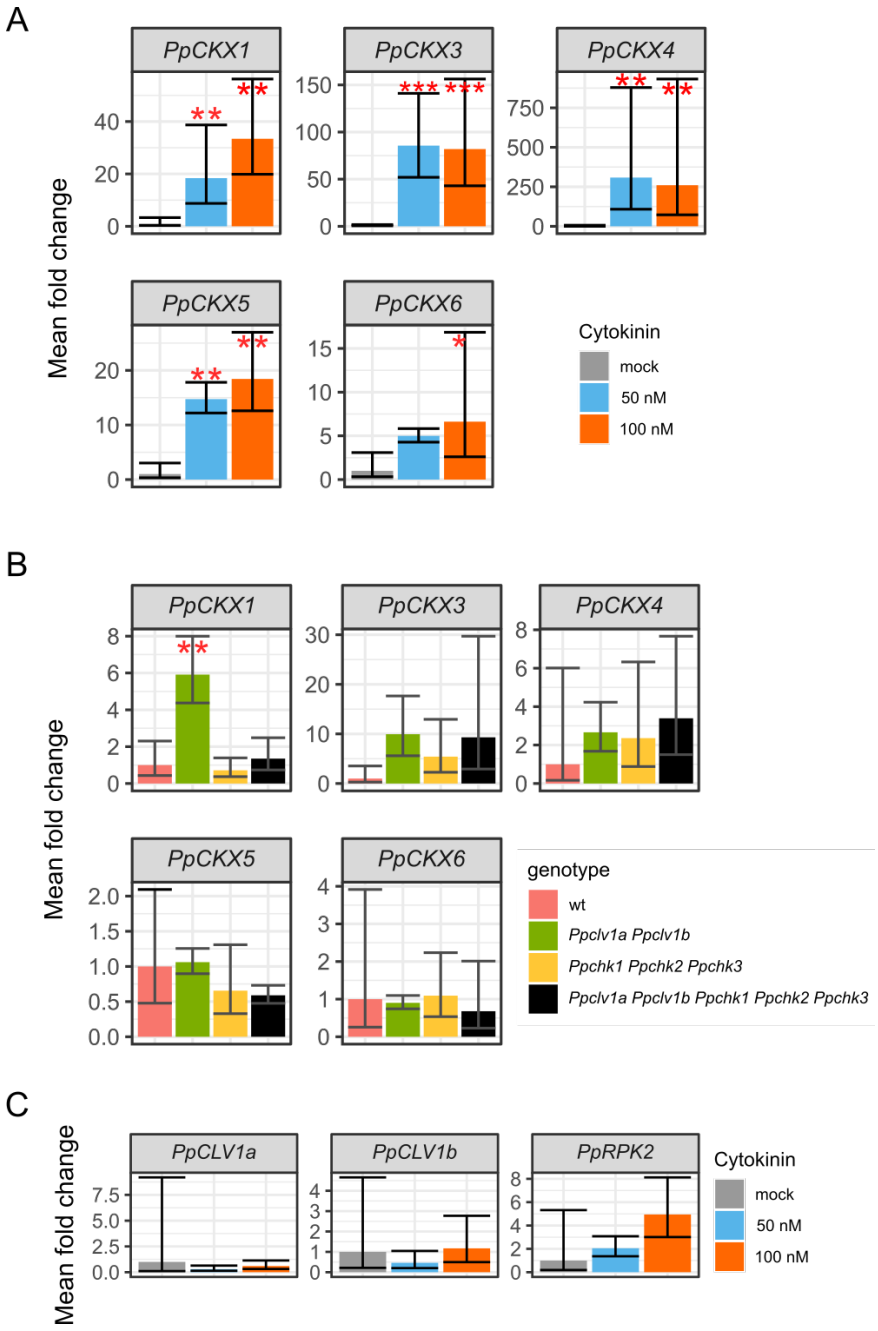

Supplemental Figure 11: Gene expression analysis testing cytokinin, *Pp*CLV1, and *Pp*RPK2 interactions. A) qPCR-data testing the change in expression of five *PpCKX* genes in response to growth on cytokinin. All *PpCKX* genes tested were upregulated, although *PpCKX6* weekly so. B) *PpCKX* gene expression was used as an indicator of cytokinin transcriptional response. *PpCKX1* expression was increased in *Ppclv1a Ppclv1b,* but unchanged in *Ppclv1a Ppclv1b Ppchk1 Ppchk2 Ppchk3*, supporting a role for *PpCLV1* in inhibiting cytokinin response. However, other *PpCKX genes* tested did not display this same trend. C) Expression levels of *PpCLV1a, PpCLV1b*, and *PpRPK2* were unchanged due to growth on cytokinin.